frontiers in Immunology

ORIGINAL RESEARCH
published: 07 April 2021
doi: 10.3389/fimmu.2021.653464

Omega-3 Polyunsaturated Fatty Acid Intervention Against Established Autoimmunity in a Murine Model of Toxicant-Triggered Lupus

James J. Pestka[1,2,3], Peyman Akbari[2,3,4], Kathryn A. Wierenga[3,5], Melissa A. Bates[2,3], Kristen. N. Gilley[2], James G. Wagner[3,4], Ryan P. Lewandowski[4], Lichchavi D. Rajasinghe[2,3], Preeti S. Chauhan[2,3], Adam L. Lock[6], Quan-Zhen Li[7] and Jack R. Harkema[3,4]**

[1] Department of Microbiology and Molecular Genetics, Michigan State University, East Lansing, MI, United States, [2] Department of Food Science and Human Nutrition, East Lansing, MI, United States, [3] Institute for Integrative Toxicology, Michigan State University, East Lansing, MI, United States, [4] Department of Pathobiology and Diagnostic Investigation, Michigan State University, East Lansing, MI, United States, [5] Department of Biochemistry and Molecular Biology, Michigan State University, East Lansing, MI, United States, [6] Department of Animal Science, Michigan State University, East Lansing, MI, United States, [7] Department of Immunology and Internal Medicine, University of Texas Southwestern Medical Center, Dallas, TX, United States

OPEN ACCESS

Edited by:
Emeir McSorley,
Ulster University, United Kingdom

Reviewed by:
Philip Calder,
University of Southampton, United Kingdom
Saame Raza Shaikh,
University of North Carolina at Chapel Hill, United States

***Correspondence:**
James J. Pestka
pestka@msu.edu
Jack R. Harkema
harkemaj@msu.edu

Specialty section:
This article was submitted to Nutritional Immunology, a section of the journal Frontiers in Immunology

Received: 14 January 2021
Accepted: 08 February 2021
Published: 07 April 2021

Citation:
Pestka JJ, Akbari P, Wierenga KA, Bates MA, Gilley KN, Wagner JG, Lewandowski RP, Rajasinghe LD, Chauhan PS, Lock AL, Li Q-Z and Harkema JR (2021) Omega-3 Polyunsaturated Fatty Acid Intervention Against Established Autoimmunity in a Murine Model of Toxicant-Triggered Lupus. Front. Immunol. 12:653464. doi: 10.3389/fimmu.2021.653464

Workplace exposure to respirable crystalline silica dust ($cSiO_2$) has been etiologically linked to the development of lupus and other human autoimmune diseases. Lupus triggering can be recapitulated in female NZBWF1 mice by four weekly intranasal instillations with 1 mg $cSiO_2$. This elicits inflammatory/autoimmune gene expression and ectopic lymphoid structure (ELS) development in the lung within 1 week, ultimately driving early onset of systemic autoimmunity and glomerulonephritis. Intriguingly, dietary supplementation with docosahexaenoic acid (DHA), an ω-3 polyunsaturated fatty acid (PUFA) found in fish oil, beginning 2 week prior to $cSiO_2$ challenge, prevented inflammation and autoimmune flaring in this novel model. However, it is not yet known how ω-3 PUFA intervention influences established autoimmunity in this murine model of toxicant-triggered lupus. Here we tested the hypothesis that DHA intervention after $cSiO_2$-initiated intrapulmonary autoimmunity will suppress lupus progression in the NZBWF1 mouse. Six-week old NZWBF1 female mice were fed purified isocaloric diet for 2 weeks and then intranasally instilled with 1 mg $cSiO_2$ or saline vehicle weekly for 4 consecutive weeks. One week after the final instillation, which marks onset of ELS formation, mice were fed diets supplemented with 0, 4, or 10 g/kg DHA. One cohort of mice (n = 8/group) was terminated 13 weeks after the last $cSiO_2$ instillation and assessed for autoimmune hallmarks. A second cohort of mice (n = 8/group) remained on experimental diets and was monitored for proteinuria and moribund criteria to ascertain progression of glomerulonephritis and survival, respectively. DHA consumption dose-dependently increased ω-3 PUFA content in the plasma, lung, and kidney at the expense of the ω-6 PUFA arachidonic acid. Dietary intervention with high but not low DHA after $cSiO_2$ treatment suppressed or delayed: (i) recruitment of T cells and B cells to the lung, (ii) development of pulmonary ELS, (iii) elevation of a wide spectrum of plasma autoantibodies associated with lupus and other autoimmune diseases, (iv) initiation

and progression of glomerulonephritis, and (v) onset of the moribund state. Taken together, these preclinical findings suggest that DHA supplementation at a human caloric equivalent of 5 g/d was an effective therapeutic regimen for slowing progression of established autoimmunity triggered by the environmental toxicant $cSiO_2$.

Keywords: systemic lupus erythematosus, NZBWF1, ω-3 polyunsaturated fatty acid, silica, docosahexaenoic acid, ectopic lymphoid structure, glomerulonephritis, autoantibody

INTRODUCTION

Systemic lupus erythematosus (lupus) is a chronic and debilitating autoantibody (AAb)-mediated systemic autoimmune disease affecting numerous organs including the kidney, lung, heart, skin, and brain (1). Patients with lupus characteristically have recurring cycles of flaring and remission that, over the long term, can result in irreversible organ damage. Environmental agents can contribute to onset, flaring, and progression of autoimmunity in genetically predisposed individuals (2). A prototypical example of an environmental autoimmune trigger is respirable crystalline silica dust ($cSiO_2$), which is commonly inhaled by workers in mining, construction, and ceramics industries worldwide (3). Occupational exposure to $cSiO_2$ has been etiologically associated with increased risk for the development and recurrent manifestation of lupus and other human autoimmune diseases (4–6), raising the need for preventive or therapeutic interventions for exposed workers.

$cSiO_2$ triggered autoimmune flaring can be recapitulated by introducing the particle to lungs of mouse models of human lupus (7–13). Specifically relevant to the present investigation is the widely used lupus-prone female New Zealand Black White (F1) (NZBWF1) mouse, which typically displays autoantibody production early in life, glomerulonephritis and proteinuria at approximately age 34 weeks, and succumbs to the disease by age 52 week (14). When this model is subjected to 4 weekly intranasal instillations with 1 mg $cSiO_2$, latency to onset for glomerulonephritis is reduced by 12 week (12, 13). Prior to glomerulonephritis onset, instilled $cSiO_2$ evokes in these mice severe pulmonary pathology (i.e., alveolitis) that includes persistent alveolar accumulation of particle-laden macrophages, monocytes, necrotic phagocytic cells, nuclear and cytoplasmic debris, and neutrophilic inflammation. Additionally, there is accumulation of large numbers of T- and B-lymphoid cells, as well as IgG-secreting plasma cells, indicative of pathological ectopic lymphoid structures (ELS). Consistent with persistent particle-induced pulmonary inflammation and ELS neogenesis, lung lavage fluid and blood plasma from $cSiO_2$-exposed mice exhibit elevated concentrations of proinflammatory cytokines, chemokines, and autoantibodies. Collectively, these findings support the contention that the lung functions as a nexus for $cSiO_2$-triggered systemic autoimmune flaring and glomerulonephritis in NZBWF1 mice.

Lifestyle factors such as diet can also attenuate or potentiate autoimmunity. One potentially promising dietary intervention against lupus is the increased intake of the marine ω-3 polyunsaturated fatty acids (PUFAs) docosahexaenoic acid (C22:6 ω-3; DHA) and eicosapentaenoic acid (C20:5 ω-3; EPA) (15). Specifically, consumption of ω-3 PUFAs may ameliorate chronic inflammation and autoimmunity by (i) altering membrane function, (ii) modulating gene expression, (iii) competition with inflammatory ω-6 PUFA-generated eicosanoids, and iv) functioning as substrates for metabolism to pro-resolving mediators [reviewed in (16–18)]. Both preclinical (19–21) and clinical studies (18, 22–24) suggest that ω-3 PUFAs might be used to prevent onset of or counter ongoing lupus symptoms, including nephritis.

The specific use of ω-3 PUFAs as a preventive approach against $cSiO_2$-triggered autoimmune flaring was demonstrated in a recent study in which female NZBWF1 mice consumed purified isocaloric diets supplemented with DHA at 0, 4, and 10 g/kg (13). These concentrations reflect on a caloric basis, human equivalent doses (HEDs) of 0, 2, and 5 g/d, respectively. DHA supplementation dramatically suppressed $cSiO_2$-triggered B- and T-cell, follicular dendritic cell (FDC), and IgG^+ plasma cell appearance in the lungs over the course of the experiment. Notably, pulmonary transcriptomic signatures of $cSiO_2$-treated mice fed control diet reflected progressive amplification of inflammation-, chemokine-, and interferon (IFN)-related gene pathways, all of which were dose-dependently inhibited by DHA (25). Protein microarray profiling has further revealed that DHA feeding dose-dependently inhibited $cSiO_2$-induced AAb responses against a multitude of lupus-associated autoantigens (AAgs), including histones, DNA, Smith antigen, complement, ribonucleoprotein, Ro/SSA, and La/SSB (26). Importantly, $cSiO_2$-triggered glomerulonephritis and lymphoid cell accumulation in the renal cortex at 13 weeks post-instillation (PI) was prevented by DHA consumption (13).

Collectively, the above-described studies establish that DHA has potent prophylactic effects against $cSiO_2$-triggered lupus in NZBWF1 mice. From a translational perspective, it is now imperative to understand how therapeutic ω-3 PUFA intervention after autoimmunity induction by $cSiO_2$ influences subsequent disease progression in this lupus model. To address this question, we tested here the hypothesis that DHA intervention after $cSiO_2$-initiated intrapulmonary autoimmunity will suppress lupus progression in the NZBWF1 mouse. Our results demonstrated that supplementation with DHA at 5 g/d but not 2 g/d DHA, after established pulmonary autoimmunity, was therapeutically efficacious in delaying $cSiO_2$-induced systemic autoimmunity, glomerulonephritis, and mortality.

TABLE 1 | Formulations of experimental diets[a].

	Experimental Diet		
	CON	low DHA[e]	high DHA[f]
Macronutrient	(g/kg total diet)		
Carbohydrates			
Corn Starch	398	398	398
Maltodextrin (Dyetrose)	132	132	132
Sucrose	100	100	100
Cellulose	50	50	50
kcal (% of total)	63.2	63.2	63.2
Proteins			
Casein	200	200	200
L-Cysteine	3	3	3
kcal (% of total)	19.7	19.7	19.7
Fats[a]			
Corn Oil[b]	10	10	10
High-Oleic Safflower Oil[c]	60	50	35
DHA-enriched Algal Oil[d]	0	10	25
kcal (% of total)	17.1	17.1	17.1
Other			
AIN93G Mineral Mix	35	35	35
AIN93G Vitamin Mix	10	10	10
Choline Bitartrate	3	3	3
TBHQ Antioxidant	0.01	0.01	0.01

Values shown are the mass amounts (g) per kg diet. [a]Based on oil composition reported by the manufacturer; [b]Corn oil contained 612 g/kg linoleic acid and 26 g/kg oleic acid; [c]high-oleic safflower oil contained 750 g/kg oleic acid and 140 g/kg linoleic acid; [d]Algal oil contained 395 DHA g/kg and 215 g oleic acid /kg; [e]4g/kg diet, calorically equivalent to human DHA consumption of 2 g/d; [f]10 g/kg diet, calorically equivalent to human DHA consumption of 5 g/d.

TABLE 2 | Fatty acid content of experimental diets.

		Experimental Diet		
		CON	low DHA	high DHA
Common Name	**Formula**	(% total fatty acids)		
Myristic	C14:0	0.31 ±0.00	1.47 ±0.04	3.38 ±0.56
Palmitic	C16:0	4.46 ±0.00	5.13 ±0.04	5.86 ±0.30
Palmitoleic	C16:1ω7	0.07 ±0.00	0.31 ±0.01	0.70 ±0.11
Stearic	C18:0	1.59 ±0.00	1.44 ±0.00	1.27 ±0.03
Elaidic	C18:1t	0.172 ±0.00	0.11 ±0.00	0.11 ±0.01
Oleic	C18:1ω9	49.05 ±0.06	44.06 ±0.20	36.81 ±2.42
Linoelaidic	C18:2ω6t	0.09 ±0.00	0.08 ±0.01	0.08 ±0.00
Linoleic	C18:2ω6	12.96 ±0.06	12.17 ±0.01	10.08 ±0.36
Arachidic	C20:0	0.27 ±0.00	0.24 ±0.00	0.20 ±0.01
gamma-Linolenic	C18:3ω6	0.01 ±0.00	0.01 ±0.00	0.01 ±0.00
Eicosenoic	C20:1ω9	019 ±0.00	0.17 ±0.00	0.15 ±0.01
alpha-Linolenic	C18:3ω3	0.23 ±0.01	0.21 ±0.00	0.19 ±0.00
Eicosadienoic	C20:2ω6	0.03 ±0.00	0.03 ±0.00	0.04 ±0.01
Behenic	C22:0	0.19 ±0.00	0.18 ±0.00	0.17 ±0.00
Arachidonic	C20:4ω6	0.00 ±0.00	0.00 ±0.00	0.01 ±0.00
Lignoceric	C24:0	0.13 ±0.00	0.12 ±0.00	0.11 ±0.00
Eicosapentaenoic	C20:5ω3	0.00 ±0.00	0.01 ±0.00	0.01 ±0.00
Nervonic	C24:1ω9	0.11 ±0.00	0.09 ±0.00	0.07 ±0.00
Docosapentaenoic ω3	C22:5ω3	0.00 ±0.00	0.07 ±0.00	0.17 ±0.03
Docosahexaenoic	C22:6ω3	0.00 ±0.00	4.07 ±0.11	10.59 ±1.82
∑ SFA		9.92 ±0.01	8.41 ±0.08	10.82 ±0.82
∑ MUFA		70.77 ±0.09	44.76 ±0.19	37.85 ±2.32
∑ ω-6 PUFA		18.70 ±0.08	12.30 ±0.00	10.21 ±0.35
∑ ω-3 PUFA		0.34 ±0.00	4.36 ±0.11	10.96 ±1.85
ω 6: ω 3 ratio		55.38 ±0.38	2.82 ±0.07	0.95 ±0.19

Data presented as percent of total fatty acids as measured by GLC. Data are mean ± SEM, n = 2.

MATERIALS AND METHODS

Mice

This study was approved by the Institutional Animal Care and Use Committee at Michigan State University (AUF #01/15-021-00). Female lupus-prone NZBWF1 mice at age 6-week were obtained from Jackson Laboratories (Bar Harbor, ME), assigned randomly to experimental groups, housed four per cage, and given free access to food and water throughout the experiment. Animal facilities were maintained at constant temperature (21–24°C) and constant humidity (40–55%) with a 12 h light/dark cycle.

Diets

Three diet formulations were employed that were based on the purified American Institute of Nutrition (AIN)-93G diet containing 70 g/kg fat that was designed for optimal rodent nutrition (27) (**Table 1**). Each diet contained 10 g/kg corn oil to ensure adequate basal essential fatty acids. The control diet (CON) contained 60 g/kg high-oleic safflower oil (Hain Pure Food, Boulder, CO). For DHA diets, high-oleic safflower oil was substituted with 10 g/kg (low DHA) or 25 g/kg (high DHA) microalgal oil containing 40% DHA (DHASCO; provided by Dr. Kevin Hadley, DSM Nutritional Products, Columbia MD). Resultant experimental diets contained 0.4 and 1.0% DHA which reflect HEDs of 2 and 5 g per day, respectively. Final fatty acid concentrations of experimental diets are shown in **Table 2**. Experimental diets were prepared weekly and stored at −20°C until use to preclude lipid oxidation. Fresh diet was supplied *ad libitum* to mice every two days.

$cSiO_2$ Preparation

Min-U-Sil-5 (1.5-2.0 μm average particle size, U.S. Silica, Berkeley Springs, WV) was prepared as previously described (28) by suspending in 1M HCl for 1 h at 100°C. After cooling, $cSiO_2$ was washed with sterile water three times and dried at 200°C overnight. Stock suspensions were prepared fresh in phosphate buffered saline (PBS) before exposure, sonicated, and vortexed for 1 min prior to intranasal instillation.

Experimental Design

The overall experimental design of this study is depicted in **Figure 1**. Briefly, 64 6-week old female NZBWF1 mice were maintained on CON diet for 7 week. At age 8-week, mice were

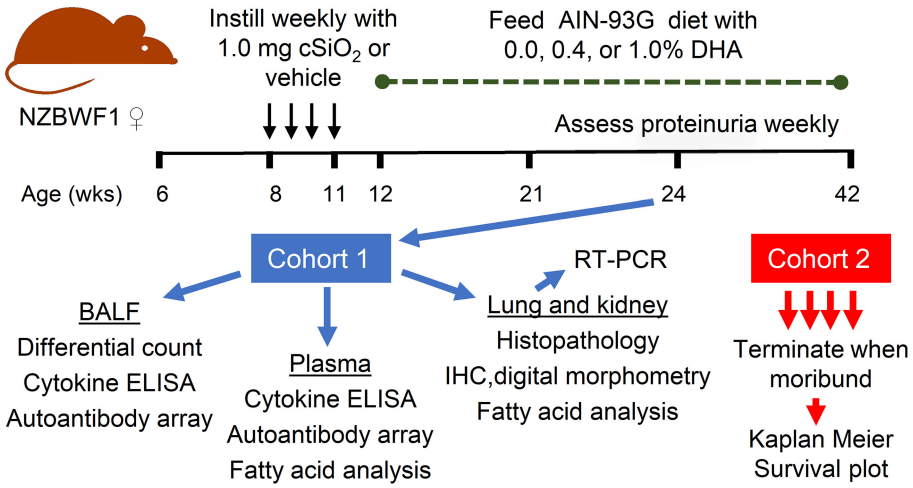

FIGURE 1 | Experimental design. Female NZBWF1 were obtained at 6 week of age and initiated on AIN-93G diet containing 0.0% DHA. At age 8 week, mice were intranasally instilled with 1.0 mg $cSiO_2$ or Veh once per week for 4 weeks. One week following the final $cSiO_2$ instillation, animals were either maintained on the control diet or fed diets containing 0.4 or 1% DHA (w/w). Eight animals per exposure/diet group (cohort 1) were sacrificed at 24 weeks, at which time BALF was collected for differential cell counts, cytokine ELISAs, and assessment of autoantibodies; plasma collected for cytokine ELISAs, assessment of autoantibodies, and fatty acid analysis; lungs and kidneys collected for histopathology, IHC and digital morphometry, RT-PCR, and fatty acid analysis. The remaining 8 animals per exposure/diet group (cohort 2) were monitored until moribund, at which point they were humanely euthanized. During this time, proteinuria was assessed weekly as a measure of disease progression.

anesthetized with 4% isoflurane and intranasally instilled with 1.0 mg $cSiO_2$ in 25 µl PBS ($n = 48$) or 25µl PBS vehicle (Veh) ($n = 16$) as described previously (12). Treatments were repeated weekly for 4 week s. This dosing regimen reflects approximately one half of the human lifetime permissible exposure level for $cSiO_2$ at the recommended Occupational Safety and Health Administration limit (29). Experimental diets were initiated 1 week PI which, as reported previously (13), corresponds with the onset of pulmonary autoimmunity reflected by ELS development. Groups of mice were assigned to diets as follows: (i) Veh-treated mice fed CON diet (Veh/CON), $n = 16$), (ii) $cSiO_2$-treated mice fed CON diet ($cSiO_2$/CON, $n = 16$), (iii) $cSiO_2$-treated mice fed low DHA diet ($cSiO_2$/low DHA, $n = 16$), and (iv) $cSiO_2$-treated mice fed high DHA diet ($cSiO_2$/high DHA, $n = 16$). Mice were divided into two equivalent cohorts and maintained on assigned diets until the end of each respective experiment.

Experimental Cohort 1 mice ($n = 8$/group) were terminated 12 weeks after the last $cSiO_2$ instillation. This termination time corresponds with robust autoimmune pathogenesis in the lung, systemic autoimmunity, and initiation of glomerulonephritis observed previously in NZBWF1 mice subjected to the above $cSiO_2$ exposure regimen (12, 13, 30). Animals were anesthetized by intraperitoneal injection with 56 mg/kg body weight sodium pentobarbital and euthanized by exsanguination via the abdominal aorta. Blood was obtained with heparin-coated syringes and centrifuged at 3500 *x* g for 10 min at 4°C to obtain plasma, which was stored at−80°C for fatty acid analyses and AAb microarray. Bronchoalveolar lavage fluid (BALF) was collected from whole lungs and centrifuged at 2400 *x* g for 15 min as described previously (31). The cell fraction was subjected to inflammatory cell differential analysis and the

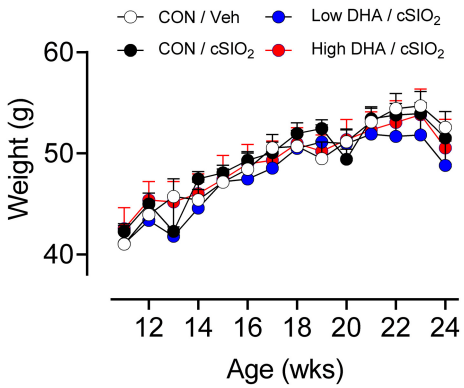

FIGURE 2 | Body weight change in NZBWF1 mice is not affected by $cSiO_2$ treatment and experimental diets. Animals in Cohort 1 were weighed weekly following the final $cSiO_2$ instillation. Data presented as mean± SEM. Differences between CON/Veh and CON/$cSiO_2$ were assessed by Student's *T*-test. Low DHA/$cSiO_2$ and high DHA/$cSiO_2$ were compared to CON/$cSiO_2$ using one-way ANOVA followed by Dunnett's *post-hoc* test. At each time point, we observed no significant differences between treatment groups.

supernatant fraction was stored at−80°C for cytokine ELISAs and autoantibody microarray. After lavage, the right lung lobes were removed, frozen in liquid nitrogen, and stored at−80°C for fatty acid analysis and FDC immunohistochemistry (IHC). Caudal lung lobes were removed, held in RNAlater (Thermo Fisher Scientific, Wilmington, DE) for 16 h at 4°C, and then stored at−80°C until RNA isolation. The left lung lobe was fixed with 10% neutral buffered formalin (Fisher Scientific, Pittsburgh, PA) at constant pressure (30 cm H_2O) for minimum of 1 h and

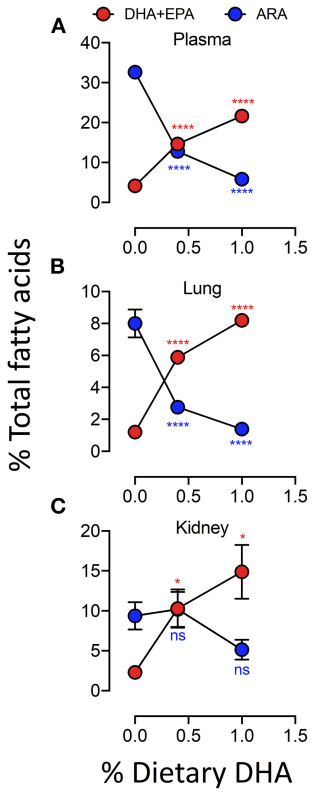

FIGURE 3 | Experimental diets influence the DHA and ARA concentrations in kidney, lung and plasma. Incorporation of EPA and DHA in the plasma **(A)** and tissues **(B,C)** increased in a dose-dependent manner that coincided with a reduction in ARA. Data presented as mean ± SEM. Fatty acid levels from animals fed the low-and high-DHA diets were compared to animals fed the CON diet. Statistical comparisons were performed as described in the Methods section. *$p < 0.05$, ****$p < 0.0001$, ns = not significant. Asterisk/text color corresponds to fatty acid data being analyzed (ARA, red; EPA+DHA, blue).

stored in fixative until further processing for histology and B- and T-cell IHC. The right kidney was excised, and the cranial portion fixed in 10% neutral buffered formalin for 24 h for histopathology and IHC. The left kidney was frozen at−80°C until fatty acid analysis.

Experimental Cohort 2 mice (n = 8/group) remained on experimental diets to monitor glomerulonephritis progression and survival. Mice were assessed weekly for proteinuria using dipsticks (Cortez Diagnostics, Inc., Calabasas, CA). They were further evaluated daily for established moribund criteria that included weight loss, inactivity, ruffled fur, and temperature drop (32). After reaching a moribund state, individual mice in this cohort were humanely euthanized as described for Cohort 1.

Fatty Acid Analyses

Gas liquid chromatography (GLC) analysis of fatty acids in diet and plasma was performed at OmegaQuant Analytics, LLC (Sioux Falls, SD) which is an independent CLIA-certified laboratory. Fatty acid concentrations of lung and kidney were determined at Michigan State University using a modification of a direct transesterification method (33) as reported previously (34). Fatty acid data were presented as percent (w/w) of fatty acids detected with a chain length between 10 and 24 carbon atoms. The lower limit of detection was <0.001 g/100 g fatty acids. The ω-3 HUFA score and %EPA+DHA were determined for tissue samples. The ω-3 HUFA score is the sum of EPA (C20:5ω3), DPA (C22:5ω3), and DHA (C22:6ω3) as a percentage of the most abundant HUFAs (C20:5ω3, C22:5ω3, C22:6ω3, C20:3ω6, C20:4ω6, C22:4ω6, C22:5ω6, C20:3ω9) (35). The %EPA+DHA was calculated by taking the sum of EPA and DHA as a percent of total fatty acids (36). In red blood cells, this value is referred to as Omega 3 Index.

BALF Cellularity

BALF cell pellets were resuspended in PBS and total leukocyte numbers were measured using a hemocytometer. Cytological slides were prepared by centrifugation at 40 x g for 10 min and stained with Diff-Quick (ThermoFisher). Differential cell counts of macrophages, neutrophils, eosinophils, and lymphocytes were determined from a minimum of 200 cells in cytospin slides.

Cytokine Analyses

DuoSets (R&D Systems, Minneapolis, MN) were used to analyze BALF supernatants for TNF-α, MCP-1, and B-cell activating factor (BAFF) according to manufacturer's instructions.

Histopathology of Lung and Kidney

Randomly oriented, serial sections of formalin-fixed left lung lobes were routinely processed and embedded in paraffin. Tissue sections (5 μm thickness) were deparaffinized and stained with hematoxylin and eosin (H&E) for light microscopic examination of histopathology. Severity of lung lesions were scored semi-quantitatively by a board certified veterinary pathologist without knowledge of individual animal exposure history (i.e., in a blinded manner). Scoring of histopathology included the amount of: (a) lymphoid aggregates within perivascular and peribronchiolar regions; (b) ELS; (c) alveolar proteinosis; (d) alveolitis (defined as the increased accumulation in the alveolar parenchyma of neutrophils, lymphocytes, and mononuclear/macrophages); (e) alveolar type II epithelial cell hyperplasia; and (f) mucous cell metaplasia in bronchiolar epithelium. Individual lungs were semi-quantitatively graded for these lesions as % of total pulmonary tissue examined based on the following criteria: (0) no changes compared to control mice; (1) minimal (<10%); (2) slight (10–25%); (3) moderate (26–50%); (4) severe (51–75%); or (5) very severe (>75%) of total area affected.

Fixed kidneys were similarly processed for light microscopic examination and tissue sections were stained with H&E or Periodic acid-Schiff and hematoxylin (PASH). Severity of lupus nephritis was evaluated in a blinded manner by the board-certified veterinary pathologist using a modified International Society of Nephrology/Renal Pathology Lupus Nephritis Classification system (37). Renal histopathology was semi-quantitatively graded as follows: (0) no tubular proteinosis and normal glomeruli; (1) mild tubular proteinosis with multifocal segmental proliferative glomerulonephritis and

TABLE 3 | Plasma fatty acid content of experimental groups.

		Experimental Group			
		Veh/CON	$cSiO_2$/CON	$cSiO_2$/low DHA	$cSiO_2$/high DHA
Common Name	**Formula**	(% of total fatty acids)			
Myristic	C14:0	0.05 ±0.01	0.07 ±0.01#	0.07 ±0.02	0.11 ±0.05
Palmitic	C16:0	15.25 ±0.39	15.72 ±0.69	17.00 ±1.23	17.90 ±1.53**
Palmitoleidic	C16:1ω7t	0.02 ±0.00	0.02 ±0.01	0.02 ±0.01	0.01 ±0.01*
Palmitoleic	C16:1ω7c	1.29 ±0.19	1.42 ±0.15	1.16 ±0.20*	1.49 ±0.17
Stearic	C18:0	12.57 ±0.51	12.04 ±0.41#	11.99 ±1.32	11.02 ±1.04
Elaidic	C18:1ω9t	0.10 ±0.01	0.10 ±0.02	0.09 ±0.02	0.07 ±0.01**
Oleic	C18:1ω9c	14.39 ±0.91	17.43 ±3.17#	16.37 ±2.91	16.06 ±1.52
Linoelaidic	C18:2ω6t	0.14 ±0.01	0.15 ±0.02	0.12 ±0.02	0.10 ±0.03**
Linoleic	C18:2ω6c	10.41 ±1.53	12.32 ±1.66#	21.72 ±1.31***	22.16 ±1.71***
Arachidic	C20:0	0.03 ±0.01	0.04 ±0.01	0.05 ±0.01*	0.04 ±0.01
Gamma-linolenic	C18:3ω6	0.21 ±0.03	0.23 ±0.04	0.16 ±0.04***	0.13 ±0.03***
Eicosanoic	C20:1ω9	0.30 ±0.04	0.32 ±0.03	0.33 ±0.05	0.28 ±0.08
Linolenic	C18:3ω3	0.01 ±0.00	0.02 ±0.01	0.02 ±0.01	0.02 ±0.01
Eicosadienoic	C20:2ω6	0.12 ±0.03	0.12 ±0.01	0.24 ±0.07**	0.17 ±0.07
Benehinic	C22:0	0.39 ±0.09	0.35 ±0.09	0.27 ±0.14	0.19 ±0.10*
Dihomo-Gamma-linolenic	C20:3ω6	1.29 ±0.14	1.16 ±0.14	2.42 ±0.59**	2.03 ±0.66*
Arachidonic	C20:4ω6	37.14 ±1.96	32.63 ±4.35#	12.80 ±2.44***	5.84 ±1.31***
Lignoceric	C24:0	0.02 ±0.01	0.02 ±0.00	0.02 ±0.01	0.02 ±0.01
Eicosapentaenoic	C20:5ω3	0.03 ±0.00	0.04 ±0.01#	2.75 ±1.08**	6.70 ±2.41***
Nervonic	C24:1ω9	0.20 ±0.05	0.20 ±0.05	0.21 ±0.08	0.20 ±0.08
Adrenic	C22:4ω6	0.23 ±0.02	0.26 ±0.04	0.05 ±0.01***	0.02 ±0.01***
Docosapentaenoic ω6	C22:5ω6	1.28 ±0.12	1.15 ±0.26	0.02 ±0.01*	0.01 ±0.01***
Docosapentaenoic ω3	C22:5ω3	0.06 ±0.01	0.07 ±0.03	0.26 ±0.04***	0.42 ±0.06***
Docosahexaenoic	C22:6ω3	4.44 ±0.14	4.12 ±0.24##	11.87 ±0.54***	14.95 ±1.65***
∑ SFA		28.33 ±0.24	28.24 ±0.56	29.40 ±0.61**	29.28 ±0.75**
∑ MUFA		16.31 ±1.12	19.49 ±3.15#	18.17 ±2.78	18.11 ±1.49
∑ n-3 PUFA		4.54 ±0.13	4.25 ±0.21##	14.91 ±0.96***	22.10 ±1.40***
∑ n-6 PUFA		50.82 ±0.90	48.02 ±3.07#	37.52 ±2.29***	30.51 ±2.28***
EPA+DHA		4.47 ±0.14	4.16 ±0.24##	14.62 ±0.97***	21.65 ±1.36***
% ω3 in HUFA		10.18 ±0.44	10.83 ±1.21	49.29 ±4.89***	73.39 ±4.71***

*Determined by GLC. All fatty acids represented as percent of total fatty acids and as mean ± SEM, n = 8. Number signs indicate significantly different than Veh/CON: #p < 0.05, ##p < 0.01. Asterisks indicate significantly different than $cSiO_2$/CON: *p < 0.05, **p < 0.01, ***p < 0.001.*

occasional early glomerular sclerosis and crescent formation; (2) moderate tubular proteinosis with diffuse segmental proliferative glomerulonephritis, early glomerular sclerosis and crescent formation; and (3) marked tubular proteinosis with diffuse global proliferative and sclerosing glomerulonephritis.

Immunohistochemistry and Digital Morphometry of Lung and Kidney

Immunohistochemistry was performed as described previously by Bates et al. (12, 30). Briefly, formalin-fixed, paraffin embedded lung and kidney tissue sections were employed for identification of B cells using 1:600 rat anti-CD45R monoclonal antibody (Becton Dickinson, Franklin Lakes, NJ, catalog # 550286) and T cells using 1:250 rabbit anti-CD3 polyclonal antibody (Abcam, Cambridge, MA catalog # ab5690). FDCs were detected in frozen lung and kidney sections using 1:500 rat anti-CD21/35 monoclonal antibody (Becton Dickinson; catalog # 553817). Slides were digitally scanned using a VS110 (Olympus, Hicksville, NY) virtual slide system. At least 100 digital images were then captured at 20X magnification using systematic random sampling with NewCast software (Visiopharm, Hoersholm, Denmark). Volume densities of $CD3^+$, $CD45R^+$, or $CD21/35^+$ cells were estimated using a point grid over the randomly sampled images with the STEPnizer 1.8 Stereology Tool. The number of points landing directly on the $CD45R^+$, $CD3^+$, or $CD21/35^+$ cells were counted and the percent positive per reference area was calculated.

mRNA Expression

TriReagent (Sigma Aldrich, St. Louis, MO) was used to extract total RNA from the lung. RNA was further purified with a Zymo RNA Clean and Concentrator Kit with DNase digestion

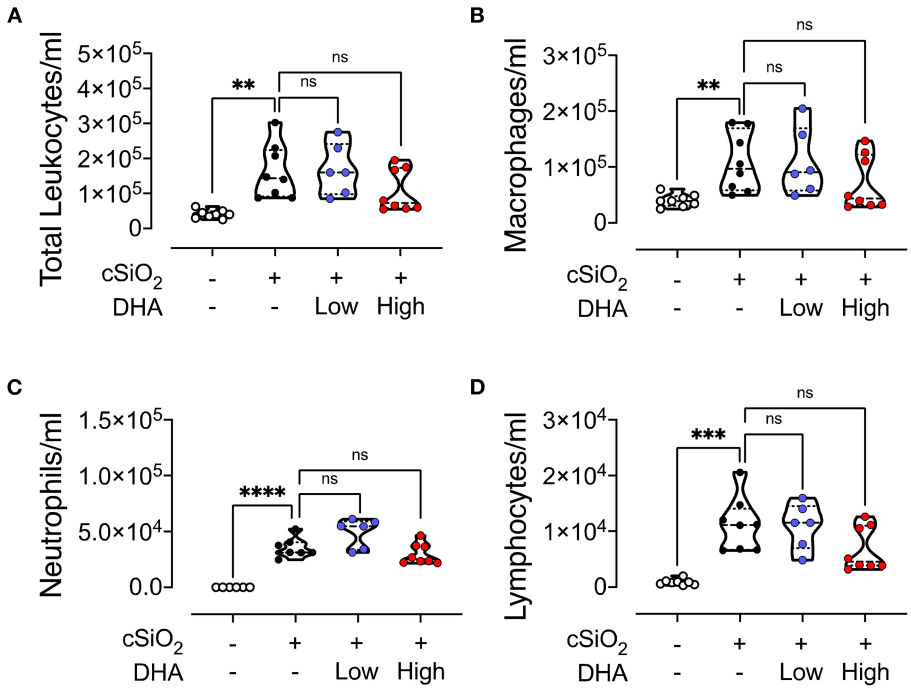

FIGURE 4 | $cSiO_2$-induced inflammatory cell recruitment into the lungs is modestly attenuated by DHA feeding. 13 week following the final $cSiO_2$ instillation, mice were necropsied and BALF collected. The BALF cell fraction was assessed for **(A)** total cells, **(B)** macrophages, **(C)** neutrophils, and **(D)** lymphocytes as measures of inflammatory cell recruitment. $cSiO_2$ significantly increased the number of each cell type in the BALF. Total leukocytes, macrophages, and lymphocytes appeared to be slightly reduced by the high DHA diet, though the difference was not significant. Statistical comparisons were performed as described in the Methods section. $^{****}p \leq 0.0001$, $^{***}p \leq 0.001$, $^{**}p \leq 0.01$, ns = not significant.

(Zymo Research, Irvine, CA, catalog #R1017). Total RNA was measured with a NanoDrop-1000 (Thermo Fisher Scientific) and reverse transcribed to cDNA at 50 ng/μl using a High-Capacity cDNA Reverse Transcription Kit (Thermo Fisher Scientific, Waltham, MA). TaqMan Assays were carried out using a SmartChip Real-Time PCR System in technical triplicates for inflammation-associated genes (*Il1a, Il1b, IL6, Il18,Tnfa, Stat2, Pparg, Nos2,Nrlp3, Nfkb, Tlr4, Tlr7, Tlr8,Tlr9, Zbp1, Arg1*), chemokine-related genes (*Ccl2, Ccl7, Ccl8, Ccl12, Cxcl1, Cxcl2, Cxcl3, Cxcl5, Cxcl9, Cxcl10*), IFN-regulated genes (*Ifit1, Irf7, IsG15, Mx1, Ifi44, Oas1a, Oas2, Oasl1, Psmb8, Rsad2, Siglec1)*, and 3 housekeeping genes (*Gapdh, Hprt, Actb*). Gene expression levels were normalized to the endogenous housekeeping genes and reported as fold change relative to the experimental control group using the $2^{-\Delta\Delta CT}$ method (38).

High-Throughput Protein Microarray AAb Profiling

High-throughput profiling of IgG AAb in BALF and plasma against a broad range of autoantigens (AAgs) was performed at the Microarray and Immune Phenotyping Core Facility at The University of Texas Southwestern Medical Center using AAg coated protein arrays (26, 39). Briefly, plasma and BALF samples were pre-treated with DNAse I to remove free-DNA, then samples were diluted at 1:50 (for plasma) or 1:25 (for BALF) and hybridized to protein array plates coated with 122 antigens and 6 controls. The antibodies binding with the antigens on plate were detected with Cy3-conjugated anti-mouse IgG (1:2000, Jackson ImmunoResearch Laboratories, PA) and fluorescent images captured with a Genepix 4200A scanner (Molecular Devices, CA). Fluorescent images were transformed to signal intensity values using GenePix 7.0 software and background-subtracted and normalized to internal controls for IgG. The processed signal intensity value for each AAb was reported as antibody score (Ab-score), which is expressed based on the normalized signal intensity and signal-to-noise ratio (SNR) using the formula:

$$\text{Ab}-\text{score} = log_2(NSI^*SNR + 1).$$

Normalized and unit variance-scaled Ab-score values were represented with heat maps, organized by unsupervised hierarchical co-clustering (HCC) generated using ClustVis (40). In heat maps, values were centered by rows; imputation was used for missing value estimation. Rows were clustered using Euclidean distance and Ward linkage. A volcano plot was generated in R Shiny online tool (https://paolo.shinyapps.io/ShinyVolcanoPlot/); *p*-values and fold change values for the volcano plots were calculated using Microsoft Excel 2016. Selected Ab-scores are reported as scatter plots, generated using GraphPad Prism version 8.3.0 for Windows (GraphPad Software, San Diego, California USA, www.graphpad.com).

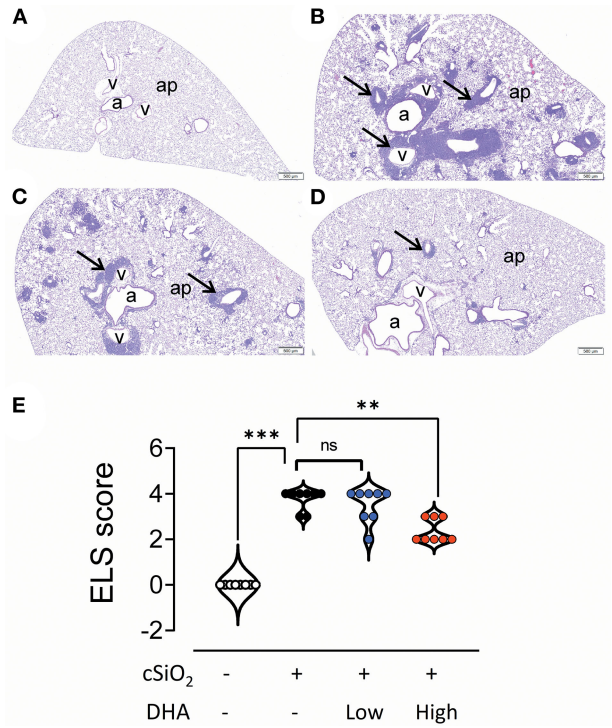

FIGURE 5 | High DHA diet reduces perivascular and peribronchiolar lymphoid aggregates in the lungs of $cSiO_2$-treated mice. Light photomicrographs of hematoxylin and eosin-stained lung tissue sections **(A–D)** from mice fed control diet and intranasally instilled with saline vehicle (Veh/CON, **A**), fed control diet and intranasally instilled with $cSiO_2$ ($cSiO_2$/CON, **B**), fed 0.4 % DHA diet starting one week after the end of the intranasal $cSiO_2$ instillations ($cSiO_2$/low DHA, **C**), or fed the 1.0% DHA diet starting one week after the end of the intranasal $cSiO_2$ instillations ($cSiO_2$/high DHA, **D**). Marked perivascular and peribronchiolar airway lymphoid cell accumulation (ectopic lymphoid structures [ELS]; arrows) observed in the lung of $cSiO_2$/CON mouse that did not receive DHA treatment **(B)**. Slightly less severe ELS formation around vessels and airways in the lung of $cSiO_2$/low DHA mouse **(C)**. Only minimal perivascular and peribronchiolar lymphoid aggregates in the lung of $cSiO_2$/high DHA mice **(D)**. b, bronchiolar airway; v, blood vessel, a, alveolar parenchyma. **(E)** Individual sections were semi-quantitatively scored for ELS using the following criteria: (0) no changes compared to control mice; (1) minimal (<10%); (2) slight (10–25%); (3) moderate (26–50%); (4) severe (51–75%); or (5) very severe (>75%) of total area affected. Horizontal lines represent mean ± SEM. Statistical comparisons were performed as described in the Methods section. $^{***}p \leq 0.001$, $^{**}p \leq 0.01$, ns = not significant.

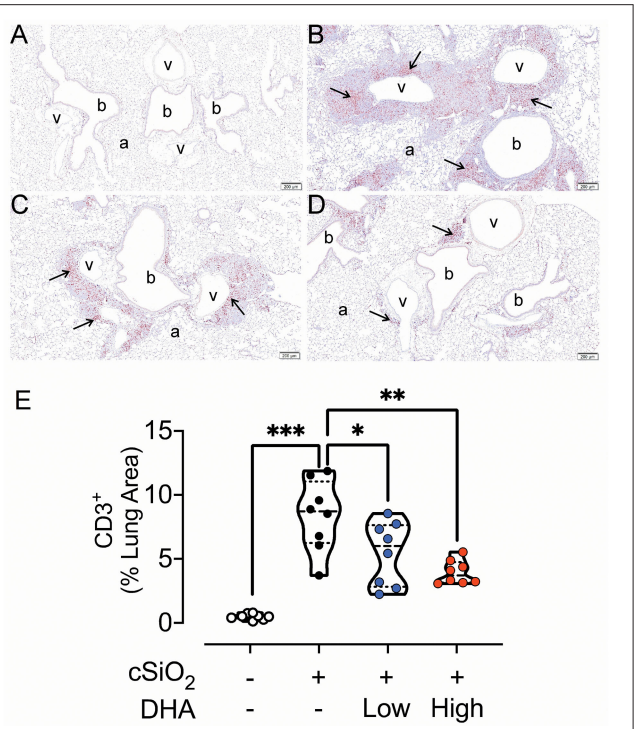

FIGURE 6 | DHA-containing diets reduce $CD3^+$ T cell infiltration in $cSiO_2$-instilled mice. Light photomicrographs of lung tissue sections immunohistochemically stained for $CD3^+$ T cells (arrows) from mice fed control diet and intranasally instilled with saline vehicle Veh/CON, **A**), fed control diet and intranasally instilled with $cSiO_2$ ($cSiO_2$/CON, **B**), fed 0.4 % DHA diet starting one week after the end of the intranasal $cSiO_2$ instillations ($cSiO_2$/low DHA, **C**), or fed the 1.0% DHA diet starting one week after the end of the intranasal $cSiO_2$ instillations ($cSiO_2$/high DHA, **D**). Marked accumulation of perivascular and peribronchiolar $CD3^+$ T cells (arrows) in lung of $cSiO_2$/CON mouse. Moderate, minimal and no accumulations of $CD3^+$ T cells around blood vessels (v) and bronchioles (b) in the lungs of $cSiO_2$/low DHA **(C)**, $cSiO_2$/high DHA **(D)**, and Veh/CON **(A)** mice, respectively. a, alveolar parenchyma. **(E)** depicts percentage of $CD3^+$ lung tissue. Statistical comparisons were performed as described in the Methods section. $^{***}p \leq 0.001$, $^{**}p \leq 0.01$, $^{*}p \leq 0.05$, ns =not significant.

Data Analysis and Statistics

All statistical analyses were performed using GraphPad Prism version 8.3.0. Data were inspected using the Grubb's outlier test (with $Q = 1\%$) to identify potential outliers and assessed for normality using the Shapiro-Wilk test ($p < 0.01$). Non-normal and semi-quantitative were analyzed using the Kruskal-Wallis nonparametric test with Dunn's *post-hoc* test (for multiple groups) or Mann-Whitney U test (for two groups). Normal data with unequal variance were analyzed using a Browns-Forsythe and Welch analysis of variance (ANOVA) with Dunnett's T3 *post-hoc* test or Welch's T-test. Data meeting both normality and equal variance assumptions were analyzed using a one-way ANOVA with Dunnett's *post-hoc* test or unpaired Student's *t*-test. Data were presented as mean ± standard error of the mean (SEM). A p-value ≤ 0.05 was considered statistically significant.

RESULTS

Body Weight and Tissue Fatty Acid Content

Female NZBWF1 mice were treated with cSiO2 and fed experimental diets as indicated in **Figure 1**. Body weight increases in Cohort 1, which were terminated 13 week post final $cSiO_2$ instillation (PI), were unaffected by $cSiO_2$ treatment or diet composition (**Figure 2**). Replacing high oleic safflower oil in AIN-93G diets with increasing amounts of DHA dose-dependently increased DHA content of the plasma (**Figure 3A**; **Table 3**), lung (**Figure 3B**; **Supplementary Table 1**), and kidney (**Figure 3C**; **Supplementary Table 2**) in NZBWF1 mice 12 week after initiating experimental diets. $cSiO_2$ exposure had negligible

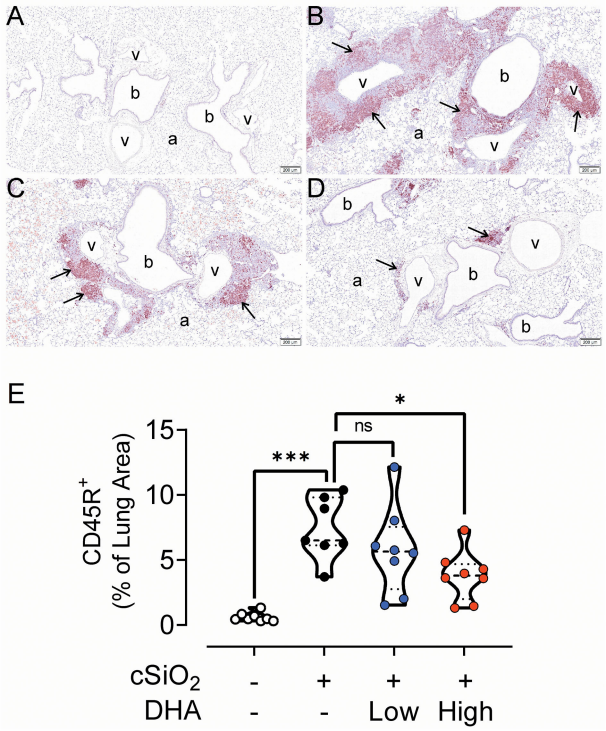

FIGURE 7 | High DHA diet reduces CD45R$^+$ B-cell infiltration in the lungs of $cSiO_2$-treated mice. Light photomicrographs of lung tissue sections immunohistochemically stained for CD45R$^+$ B cells (arrows) from mice fed control diet and intranasally instilled with saline vehicle (Veh/CON, **A**), fed control diet and intranasally instilled with $cSiO_2$ ($cSiO_2$/CON, **B**), fed 0.4 % DHA diet starting one week after the end of the intranasal $cSiO_2$ instillations ($cSiO_2$/low DHA, **C**), or fed the 1.0% DHA diet starting one week after the end of the intranasal $cSiO_2$ instillations ($cSiO_2$/high DHA, **D**). Marked perivascular and peribronchiolar B lymphoid cell accumulations (arrows) in lung of $cSiO_2$/CON mouse. Moderate, minimal and no accumulations of B lymphoid cells around blood vessels (v) and bronchioles (b) in $cSiO_2$/low DHA **(C)**, $cSiO_2$/high DHA **(D)**, and Veh/CON (**A**) mice, respectively. a, alveolar parenchyma. **(E)** depicts percentage of CD45R+ stained lung tissue. Statistical comparisons were performed between groups, as described in the Methods section. ***$p \leq 0.001$, *$p \leq 0.05$, ns = not significant.

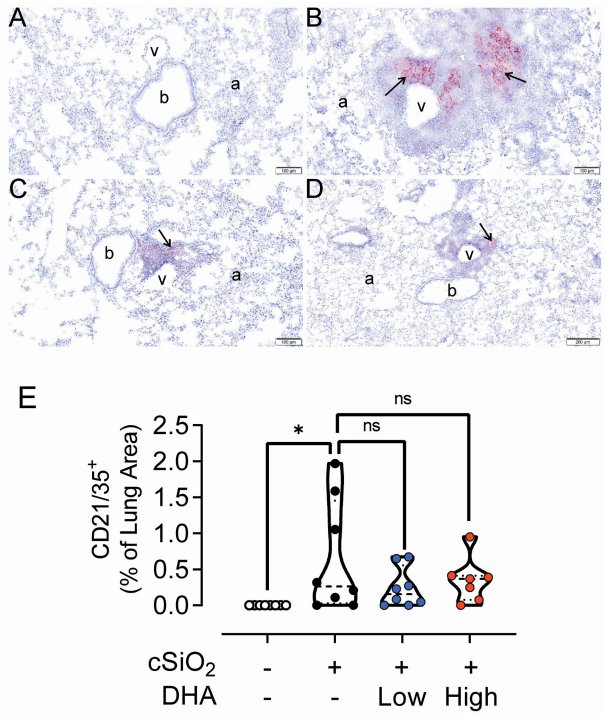

FIGURE 8 | DHA-containing diets reduce CD21/35$^+$ follicular dendritic cell (FDC) infiltration in the lungs of $cSiO_2$-treated mice. Light photomicrographs of lung tissue sections immunohistochemically stained for CD21/CD35$^+$ FDC (arrows) from mice fed control diet and intranasally instilled with saline vehicle (Veh/CON, **A**), fed control diet and intranasally instilled with $cSiO_2$ ($cSiO_2$/CON, **B**), fed 0.4% DHA diet starting one week after the end of the intranasal $cSiO_2$ instillations ($cSiO_2$/low DHA, **C**), or fed the 1.0% DHA diet starting one week after the end of the intranasal $cSiO_2$ instillations ($cSiO_2$/high DHA, **D**). Marked perivascular and peribronchiolar accumulations of follicular dendritic cells in lung of $cSiO_2$/CON mouse. Moderate, minimal and no accumulations of follicular dendritic cells around blood vessels (v) and bronchioles (b) in $cSiO_2$/low DHA **(C)**, $cSiO_2$/high DHA **(D)**, and Veh/CON **(A)** mice, respectively. a, alveolar parenchyma. **(E)** depicts percentage of CD21/35+ stained tissue. Statistical comparisons were performed between groups, as described in the Methods section. *$p \leq 0.05$, ns = not significant.

effects on tissue DHA content of CON-fed mice. Concurrently, there were nearly equivalent reductions of the ω-6 PUFA arachidonic acid (ARA), indicating that DHA replaced ARA in these tissues. Finally, EPA also increased dose-dependently in plasma (**Table 3**), lung (**Supplementary Table 1**), and kidney (**Supplementary Table 2**) with increasing concentrations of DHA in the diet. Recent isotope labeling studies have revealed increased EPA in DHA-fed rats is primarily a result of elongation/desaturation of alpha linoleic acid (ALA) to docosapentaenoic acid (DPA) mediated via feedback inhibition by DHA and, to a much lesser extent, by retroconversion of DHA (41).

BALF Cellularity and Cytokines

Intranasal instillation in Cohort 1 mice fed CON diet with $cSiO_2$ resulted in significant elevations of total leukocytes, macrophages, lymphocytes, and neutrophils in the BALF compared to vehicle-treated CON-fed mice (**Figures 4A–D**). These cell populations in $cSiO_2$/low DHA and $cSiO_2$/high DHA groups did not differ from the $cSiO_2$/CON group. $cSiO_2$ instillation of CON-fed NZBWF1 mice induced elevations in BALF of the proinflammatory cytokine TNF-α, the chemokine MCP-1, and the B cell stimulation factor BAFF, however, intervention with low or high DHA diets did not affect TNF-α, MCP-1, or BAFF responses (**Supplementary Figure 1**).

Lymphoid Cell Recruitment and ELS Development in the Lungs

No histopathology was microscopically found in the lungs of Cohort 1 Veh/CON mice (controls) that received intranasal instillations of saline vehicle alone, fed control diet and were sacrificed 13 week after the last instillation (**Figure 5A**). Lungs from $cSiO_2$/CON mice that were similarly fed and

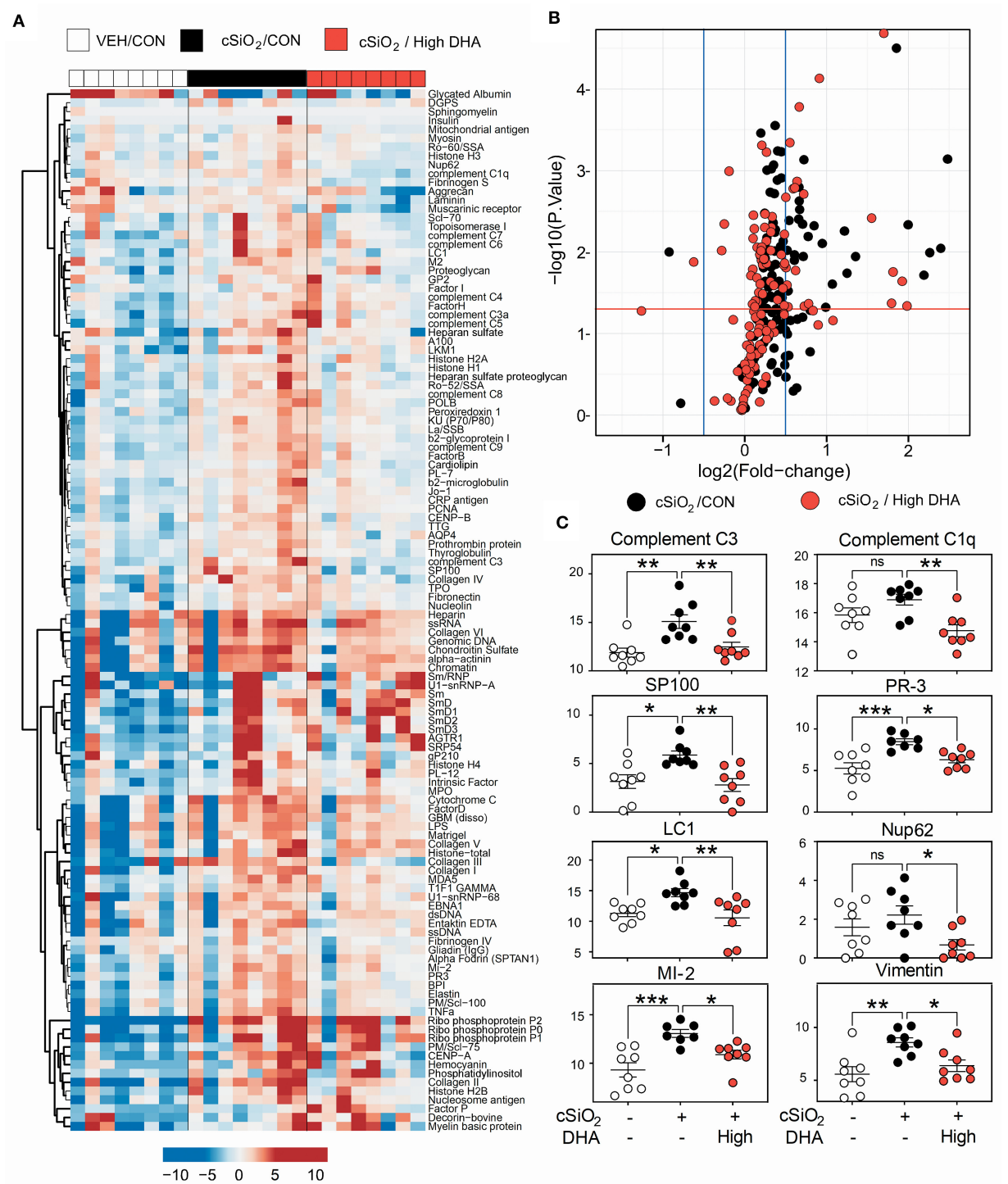

FIGURE 9 | High DHA supplementation inhibits a broad spectrum of IgG autoantibodies induced by $cSiO_2$. **(A)** Heat maps with unsupervised clustering (Euclidian distance method) of 122 AAbs depict Ab-score values for IgG expression in BALF. White, black, and red in the top key indicates the Veh/CON, $cSiO_2$/CON, and $cSiO_2$/high DHA experimental groups, respectively. Scale bar values reflect the range of variance-stabilized Ab scores, which were centered across rows. **(B)** Volcano plots depicting $cSiO_2$-induced IgG AAb responses in plasma at 13 week post final exposure in lung of $cSiO_2$-treated NZBWF1 mice. The individual AAg within each treatment group are plotted as log_2 (fold change) vs. -log_{10} (p-value). Black dots indicate $cSiO_2$/CON relative to Veh/CON treated mice; red dots indicate $cSiO_2$/high DHA relative to Veh/Con. The vertical blue lines represent the cut-off levels log_2 fold change < -0.5 or >0.5. The horizontal red line represents the cut-off levels p-values ≥ 0.05 (log10 P$\geq$ 1.2). **(C)** DHA intake suppressed $cSiO_2$-induced IgG AAb responses against selected AAgs. Data presented as mean ± SEM. Statistical comparisons were performed as described in the Methods section. $^{***}p \leq 0.001$, $^{**}p \leq 0.01$, $^{*}p \leq 0.05$, ns = not significant.

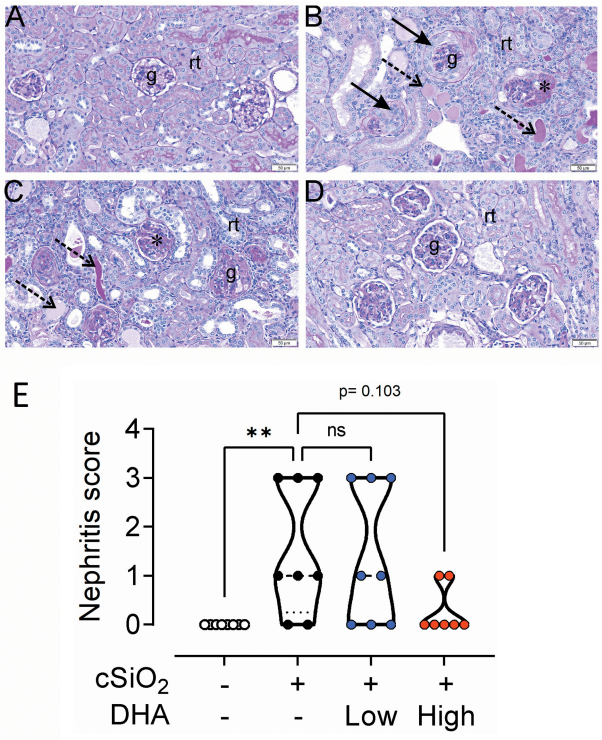

FIGURE 10 | High DHA diet slightly inhibits $cSiO_2$-triggered glomerulonephritis. Representative periodic acid Schiff-stained kidney tissue sections **(A–D)** from mice fed control diet and intranasally instilled with saline vehicle (Veh/CON; **A**), fed control diet and intranasally instilled with $cSiO_2$ ($cSiO_2$/CON; **B**), fed 0.4% DHA diet starting one week after the end of the intranasal $cSiO_2$ instillations ($cSiO_2$/low DHA; **C**), or fed 1.0% DHA diet starting one week after the end of the intranasal $cSiO_2$ instillations ($cSiO_2$/high DHA; **D**). Kidney histopathology consisting of shrunken glomerular tufts, mesangial matrix expansion, in glomeruli (asterisk), crescent-shaped masses of proliferating cells in Bowman's space (solid arrow), regenerative tubular epithelium, and tubular protein accumulation (dotted arrows) were evident only in $cSiO_2$-instilled mice that received no or low DHA treatment **(D)**. No renal histopathology was present in Veh/CON or $cSiO_2$/high DHA treatment. g, glomerulus; rt, cortical renal tubules. **(E)** Semiquantitative scoring based on histopathology conducted as described in Materials and Methods. $^{**}p \leq 0.01$, ns = not significant.

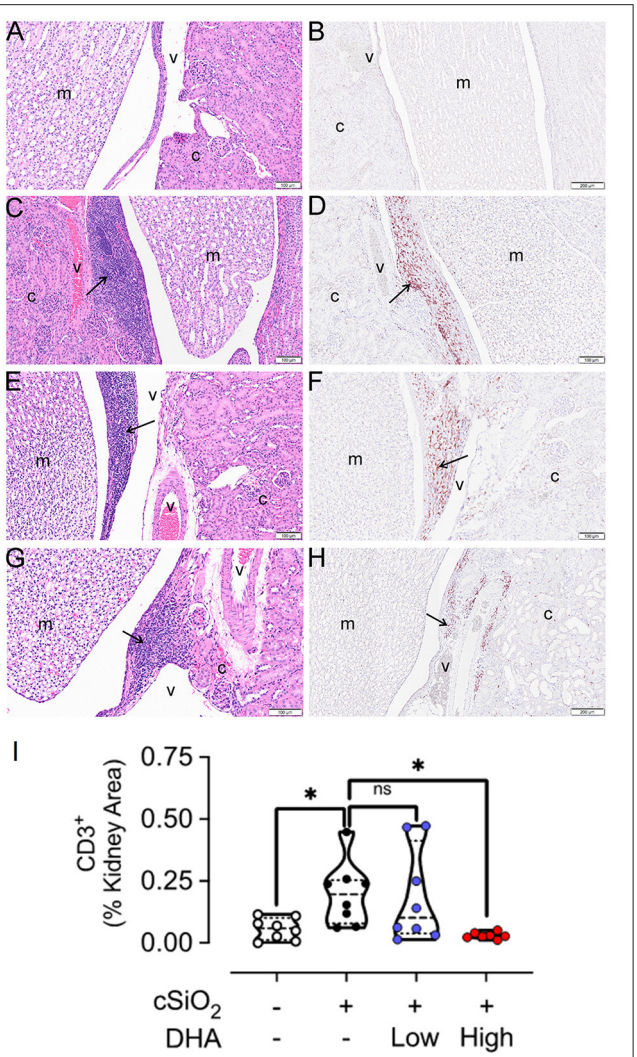

FIGURE 11 | High DHA diet suppresses $cSiO_2$-induced $CD3^+$ T cell infiltration into the kidney. Light photomicrographs of hematoxylin and eosin-stained renal tissue sections **(A,C,E,G)** from the hilar region and light photomicrographs of kidney tissue sections immunohistochemically stained (arrows) for $CD3^+$ T cells **(B,D,F,H)**. Kidneys taken from mice at 13 weeks after the final intranasal saline intranasal instillation and fed control diet (Veh/CON, **A,B**), $cSiO_2$ instillation and fed control diet ($cSiO_2$/CON, **C,D**), $cSiO_2$ instillation and fed 0.4% DHA diet ($cSiO_2$/low DHA, **E,F**), and $cSiO_2$ instillation and fed 1.0% DHA diet ($cSiO_2$/high DHA, **G,H**).Lymphoid cell accumulations (arrows) in the interstitial tissue adjacent to interlobular blood vessels (v) in the renal cortex (c) **(C,E,G)**). Marked perivascular accumulation of lymphoid cells in the renal cortex (c) from $cSiO_2$/CON mouse **(C)**. Moderate, mild and no perivascular accumulations of lymphoid cells in the kidneys of $cSiO_2$/low DHA **(E)**, $cSiO_2$/high DHA **(G)**, and Veh/CON **(A)** mice, respectively. Marked perivascular accumulation of $CD3^+$ T cells (arrows) in kidney of $cSiO_2$/CON mouse **(D)**. Moderate, minimal and no perivascular accumulations of T lymphoid cells in the kidneys of $cSiO_2$/low DHA **(F)**, $cSiO_2$/high DHA **(H)**, and Veh/CON **(B)** mice, respectively. m, medulla of the renal papilla that extends into the renal pelvis. **(I)** depicts the percentage of $CD3^+$ renal tissue. Statistical comparisons were performed as described in the Methods section. $^{*}p \leq 0.05$, ns = not significant.

sacrificed at 13 week PI had the most severe pulmonary lesions due to $cSiO_2$ (**Figure 5B**). These lesions were most prominent in the hilar region of the lung lobe. $cSiO_2$-induced histopathology consisted of conspicuous mononuclear lymphoid cell accumulations in the interstitial space surrounding small- and large-diameter blood vessels (arterial and venous) and to a lesser extent in the interstitium around bronchiolar airways (**Figure 5B**).These perivascular and peribronchiolar accumulations contained $CD3^+$ T cells (**Figures 6A,B**), $CD45R^+$ B cells (**Figures 7A,B**), $CD21^+/CD34^+$ FDC (**Figures 8A,B**) that together were morphologically consistent with ELS formation. In addition to ELS in these $cSiO_2$-instilled mice, there were adjacent areas of alveolitis characterized by alveolar infiltration of a mixed inflammatory cell population of neutrophils, monocytes/macrophages, and lymphocytes along with alveolar airspace accumulation of amorphous proteinaceous material (proteinosis), cellular/nuclear debris, and birefringent $cSiO_2$ particles within and outside of vacuolated alveolar macrophages. $cSiO_2$-induced lung lesions, especially ELS, were similar in

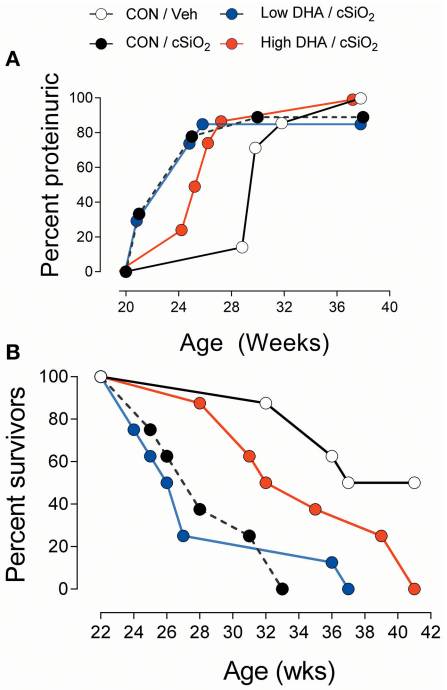

FIGURE 12 | High DHA diet delays $cSiO_2$-triggered onset of proteinuria and prolongs survival in $cSiO_2$-treated lupus-prone NZBWF1 mice. Animals in Cohort 2 were initiated on control diets 1 week following the final $cSiO_2$ instillation and animals monitored for proteinuria (≥300 mg/dl) using clinical dipsticks **(A)** and for survival using moribund criteria **(B)**.

cellular and distributional character in $cSiO_2$/low DHA and $cSiO_2$/CON mice (**Figures 5B,C,E**), but markedly less severe in $cSiO_2$/high DHA mice (**Figures 5D,E**). Consumption of high but not low DHA diet similarly reduced perivascular and peribronchiolar accumulations containing $CD3^+$ T cells (**Figures 6C–E**) and $CD45R^+$ B cells (**Figures 7C–E**) with a similar trend being evident for $CD21^+/CD34^+$ FDC (**Figures 8C–E**). The severity of alveolar proteinosis and accumulation of cellular/debris and birefringent $cSiO_2$ particles, however, were not noticeably different among the lungs of $cSiO_2$/CON, $cSiO_2$/low DHA, and $cSiO_2$/high DHA mice (**Figures 5B–D**).

mRNA Signatures in the Lungs

Repeated $cSiO_2$ exposure has been previously shown to induce expression of numerous inflammation-, chemokine-, and IFN-associated genes (42) and, furthermore, these responses can be suppressed by prophylactically feeding low and high DHA diets (25). In distinction from that preventive study, we found in Cohort 1 that DHA intervention after the insult did not impact expression of $cSiO_2$-triggered mRNA signatures associated with inflammation, chemokine production, or IFN signaling (**Supplementary Figure 2**).

IgG AAb Responses in Plasma and BALF

A vast repertoire of IgG AAbs associated with lupus and other autoimmune diseases was elicited in plasma of Cohort 1 mice following $cSiO_2$ treatment, many of which were suppressed by high DHA supplementation (**Figures 9A,B**). These included anti-complement 3 (lupus), anti-complement C1q (lupus), anti-SP100 (lupus), PR-3 (vasculitis), anti-LC-1 (autoimmune hepatitis), anti-Nup62 (primary biliary cirrhosis), anti-MI-2 (myositis), and anti-vimentin (rheumatoid arthritis) (**Figure 9C**). Although $cSiO_2$ likewise induced a diverse array of IgG AAbs in BALF, these were largely unaffected by feeding DHA (**Supplementary Figure 3**).

Glomerulonephritis and T Cell Infiltration in the Kidney

No histopathology was present in the kidneys of Veh/CON mice (**Figure 10A**). Moderate to marked membranoproliferative glomerulonephritis was evident in the $cSiO_2$/CON group (**Figure 10B**). This was characterized by thickening of PAS^+ interstitial tissue in glomeruli, hyperplasia of glomerular mesangial cells, parietal epithelial hyperplasia in Bowman's capsule (crescent formation), mixed inflammatory cell infiltration in the renal cortex (neutrophils and mononuclear cells), regenerative hyperplasia of renal tubular epithelium, and amorphous accumulation of proteinaceous and hyaline material in dilated renal tubules. Similar histopathology but of slightly less severity was evident in the kidneys of $cSiO_2$/low DHA mice (**Figure 10C**). Minimal to no renal histopathology was present in $cSiO_2$/high DHA mice (**Figure 10D**). Semiquantitative scoring indicated that there was a trend toward inhibition of $cSiO_2$ induced glomerulonephritis by high DHA supplementation (**Figure 10E**).

Cohort 1 kidneys were further subjected to cellularity assessment in H&E-stained sections (**Figures 11A,C,E,G**) and immunohistochemical localization of $CD3^+$ T cells (**Figures 11B,D,H,I**). Accumulations of renal lymphoid cells (**Figure 11A**) or $CD3^+$ cells (**Figure 11B**) were not evident in Veh/CON mice. However, in the renal cortex at the hilar region of the kidney of Veh/$cSiO_2$ mice, there were mononuclear lymphoid cell accumulations resembling ELS in interstitial tissue adjacent to interlobular blood vessels (arteries and veins) and the renal pelvis (**Figure 11C**). These increases corresponded with elevated $CD3^+$ cells (**Figure 11D**). There were less lymphoid and $CD3^+$ T cells in $cSiO_2$/low DHA mice (**Figures 11E,F**) with decreases being more marked in $cSiO_2$/high DHA mice (**Figures 11G,H**). Morphometry confirmed that $cSiO_2$ treatment induced the accumulation of $CD3^+$ T cells, which was inhibited by feeding high DHA diet (**Figure 11I**).

Proteinuria and Survival

The kidney histopathology in Cohort 1 mice was highly predictive of the development of proteinuria in Cohort 2 mice (**Figure 12A**). Proteinuria onset occurred at age 21 week in $cSiO_2$/CON and $cSiO_2$/low DHA groups, whereas proteinuria was first evident at 25 and 29 week age in $cSiO_2$/high DHA and Veh/CON groups, respectively. Further consonant with glomerulonephritis findings, Kaplan-Meier analysis of Cohort 2

revealed that median survival times for $cSiO_2$/CON, $cSiO_2$/low DHA, $cSiO_2$/high DHA, and Veh/CON groups were 28, 27, 34, and 39 week, respectively (**Figure 12B**). Thus, consumption of high DHA diet suppressed proteinuria and extended survival of $cSiO_2$-treated mice.

DISCUSSION

While an individual's genome is a critical determinant of predisposition toward autoimmunity, a multitude of lifestyle and environmental factors can potentiate or attenuate disease penetrance. Here, we investigated for the first time how dietary supplementation with the ω-3 PUFA DHA influences progression of autoimmunity initiated in NZBWF1 mice by repeated intranasal exposures to the autoimmune trigger $cSiO_2$. DHA consumption was found to dose-dependently increase DHA, and to a lesser extent, EPA, in the plasma, lung, and kidney. Supplementation with low or high DHA did not impact the inflammatory state of the lung as represented both by leukocyte numbers/profiles and cytokine concentrations in BALF and by expression of proinflammatory, chemokine, or IFN-regulated genes. However, several novel findings suggest that DHA markedly reduced progression of preexistent autoimmunity in the lung and that this ultimately impacted the systemic and renal compartments. First, provision of high DHA diet attenuated $cSiO_2$-induced T- and B cell recruitment and ELS development in the lung. Second, high DHA supplementation suppressed $cSiO_2$-triggered elevations of a wide spectrum of pathogenic AAbs in plasma. Third, mice consuming high DHA exhibited delayed onset and progression of glomerulonephritis and proteinuria. Fourth, lifespans of $cSiO_2$-instilled mice were extended in those fed high DHA as compared to those fed control diets. Finally, amelioration of $cSiO_2$ -triggered autoimmune effects and reduction in survival time were not observed in mice fed low DHA diet. Cumulatively, the results of this preclinical study support the contention that DHA supplementation at 5 g/d HED was an effective therapeutic intervention for slowing progression of established autoimmunity induced by the environmental toxicant $cSiO_2$.

Since inhaled $cSiO_2$ is inefficiently cleared from the lung, the long-term persistence of these particles causes a perpetual cycle in alveolar macrophages that includes: (i) phagocytosis, (ii) lysosomal membrane permeabilization, (iii) inflammasome activation, (iv) cell death, and (v) $cSiO_2$ release. Additional rounds of this cycle likely promote chronic unresolved inflammation in the pulmonary compartment, thereby driving the loss of immunological tolerance (43, 44). Consistent with this paradigm, intranasal instillation of NZBWF1 mice with $cSiO_2$ causes sterile inflammation in the lung characterized by leukocyte recruitment, elevated cytokines and chemokines, upregulated mRNA signatures associated with chemokines, cytokines, IFN, complement, and adhesion molecules (42). Our previous studies show that preventive feeding of NZBWF1 mice with low or high DHA diets before $cSiO_2$ instillation impairs inflammatory recruitment of macrophages, neutrophils, and lymphocytes into the lung alveolar space at 9 and 13 week PI (13). While consumption of high but not low DHA diets suppressed $cSiO_2$-induced TNF-α, MCP-1, and BAFF in BALF (30), both levels inhibit $cSiO_2$-triggered inflammatory/autoimmune gene expression at 1, 5, and 9 week PI, and to a lesser extent, at 13 week PI (25). Unlike these previously reported preventive studies, we observed here in Cohort 1 that when initiated after $cSiO_2$ treatment, neither dietary DHA level affected the overall inflammatory state of the lung relative to cell numbers, leukocyte profiles, cytokine concentrations, or gene expression. Intriguingly and consistent with earlier preventive studies (13, 30), high DHA consumption attenuated development of T-cell- and B-cell-containing ELS in the lung. One explanation for these dichotomous responses is that in the therapeutic regimen, DHA might slow inflammation at earlier time points thereby attenuating downstream ectopic lymphoid neogenesis, however, by 13 week PI, this attenuation was no longer apparent because the $cSiO_2$-driven vicious cycle of cell death and inflammation overwhelms the pro-resolving effects of ω-3 PUFAs. Nevertheless, suppression of ectopic lymphoid neogenesis was still observable. Therefore, in future investigations evaluating the therapeutic efficacy of ω-3 PUFAs in this and other preclinical models of autoimmunity, it will be important to measure inflammatory biomarkers at multiple time points and relate these to developing autoimmunity.

Because $cSiO_2$ induces cell death (45–47) and impedes efferocytosis (48), resultant dead cell accumulation and secondary necrosis likely unmasks a rich and diverse autoantigen profile in the lung that induces a broad range of AAbs. Consistent with this possibility, repeated intranasal $cSiO_2$ instillation in NZBWF1 mice a diverse repertoire of AAbs in BALF and plasma that could be delayed by preventive low and high DHA supplementation (26, 30). In the present therapeutic study, consumption of high DHA diet after $cSiO_2$ treatment also suppressed elevation of a large repertoire of pathogenic IgG AAbs in the plasma of Cohort 1 that bound autoantigens that included C1q, C3, SP100, PR-3, LC1, Nup62, MI-2, and vimentin. Interestingly, feeding either DHA diet did not affect IgG AAb responses in the BALF. A potential reason for the observed differences between DHA's effects in the systemic and pulmonary compartments is that plasma IgG AAbs might arise from B-cells that have migrated from the lung to the spleen and other lymph nodes and that increasing the membrane ω-3 PUFA content might interfere with this homing. Relatedly, Cucchi et al. (49) recently reported that EPA and DHA influence $CD4^+$ T cell motility and alter their capacity to reach target tissues by interfering with the cytoskeletal changes necessary for cell migration. Clearly, further research is needed to address whether ω-3 PUFAs similarly influence B cell motility.

Consistent with histopathological indications of glomerulonephritis and renal accumulation of T-cells in Cohort 1, mice consuming high DHA diet exhibited delayed onset and progression of proteinuria in Cohort 2. These findings are significant because glomerulonephritis is a frequent and serious organ-specific manifestation of lupus, with 10 to 30% of patients developing kidney failure (50). Various T cell subsets can activate the glomerular immune response by releasing nephritogenic cytokines or cooperating with B-cells,

macrophages, and dendritic cells (51). The observation in Cohort 1 that mice fed high DHA diet after $cSiO_2$ exposure exhibited extended lifespans compared to CON likely relates to reduced glomerulonephritis.

American diets contain many times more ω-6 PUFAs than ω-3 PUFAs, thereby skewing tissue phospholipid fatty acid content profoundly toward ω-6 PUFAs (52, 53). At the mechanistic level, increasing the ratio of the ω-3 PUFAs DHA and EPA to the ω-6 PUFA ARA in tissues can influence inflammation and autoimmune pathogenesis in numerous ways. When incorporated into the cell membrane, ω-3 PUFAs impede lipid raft formation and inhibit activation of transmembrane receptors linked to innate and adaptive immune processes (54). Intracellular and extracellular phospholipases can liberate DHA and EPA from the membrane (55, 56), enabling them to activate transmembrane receptors that interfere with proinflammatory signaling pathways (57, 58). Additionally, ω-3 PUFAs are known ligands for PPARγ, a transcription factor that can hamper NF-kB-dependent transcription of genes associated with inflammation and autoimmunity (59, 60). Furthermore, ω-6 PUFAs, including ARA, are metabolized to proinflammatory prostaglandins, thromboxanes, and leukotrienes or the pro-resolution lipoxins (61). As shown here, dietary DHA supplementation dose-dependently decreases the ARA content in plasma, lung, and kidney, thereby reducing the availability of this key substrate for generation of proinflammatory mediators.

DHA and EPA also directly compete with ω-6 PUFAs as enzymatic substrates to specialized pro-resolving mediators (SPMs) (e.g., resolvins, protectins, maresins) (62) that can impede inflammatory signaling (63, 64) and promote efferocytosis which are critical to maintaining immune tolerance (63, 64). Germaine to the present study, resolvin D1 and resolvin D2 and maresin 1 can (i) suppress cytokine production by activated $CD8^+$ T cells and $CD4^+$ T helper 1 (TH1) and TH17 cells, (ii) inhibit naïve $CD4^+$ T cell differentiation into TH1 and TH17 cells by GPR32 and ALX/FPR2 receptor-mediated down-regulation of critical transcription factors, and (iii) enhance *de novo* generation and function of $Foxp3^+$ regulatory T (Treg) cell (65). Furthermore, Crouch et al. (66) reported that in obese mice the DHA-derived SPMs 14-HDHA and 17-HDHA control B cell numbers and lower circulating IgG2c. Thus, it is tempting to speculate that in the lupus model system, the effects of dietary DHA may be driven part by the capacity of this novel family of molecules to regulate T cell subset number, B cell subset numbers, and proinflammatory antibody levels. Altogether, altering the tissue balance by increasing ω-3 PUFAs and decreasing ω-6 PUFAs likely promotes resolution over inflammation, thus preserving immunological tolerance.

As shown here, low and high DHA diets dose-dependently altered relative tissue PUFA content by increasing ω-3 PUFAs and decreasing ω-6 PUFAs, most notably ARA. We recently performed an analysis relating the red blood cell (RBC) ω-3 PUFA levels to disease severity and progression in previous studies we had performed on NZBWF1 mice supplemented with DHA on the background of three unique diets (15). Most autoimmune and inflammatory endpoints, including inflammatory gene expression, cytokine concentrations, immune cell infiltration, and AAB production negatively correlated with RBC omega-3 levels. Since these prior studies exclusively utilized prophylactic DHA supplementation, animals already had ω-3 PUFA-enriched membranes at the time of $cSiO_2$ instillation and induction of disease flaring. In the present study, therapeutic administration of the low DHA dose did not effectively suppress lupus flaring, even though this dose provided in this study achieved similar RBC ω-3 PUFA levels shown to confer moderate protection in the prophylactic supplementation model. Rather, only mice fed the high DHA diet after $cSiO_2$ showed reduced progression of ectopic lymphoid neogenesis, systemic autoimmunity, and glomerulonephritis. From a clinical perspective, this would suggest that slowing progression of established autoimmunity requires higher ω-3 PUFA intake—and subsequently, higher RBC ω-3 PUFA content—than does preventing onset of autoimmunity.

The high DHA diets equate to an HED of 5 g/d which is a realistic and safe human dose (67).Consistent with the observation here that attenuating effects were only associated with the high DHA dose, human investigations demonstrating marine ω-3 PUFA ameliorative effects on inflammatory mediators or inflammatory cell function typically have employed intakes of > 2 g/d (18). A recent meta-analysis concluded that more than 3 g/d in human clinical trials may be beneficial for lupus (23). Likewise, clinical benefits have been reported in patients with rheumatoid arthritis when consuming approximately ≥ 3.5 g/d of marine ω-3 PUFAs (18). It is therefore pertinent to ask to whether these high intakes can be achieved through diet or require taking supplements. Certain marine algae proficiently elongate shorter chain ω-3 fatty acids to DHA and EPA that make them the primary producers in the food web. Fatty fish such as mackerel and salmon consume these algae and bioconcentrate ω-3 PUFAs, and are the principal source for these fatty acids in the human diet. While a meal of oily fish such as salmon can provide 1.5 to 3 g of marine ω-3 PUFAs, consumers of the typical Western diet do not eat seafood daily. Rather, marine ω-3 PUFA consumption ranges in the tens to low hundreds of mg/d as reviewed by Calder (68). Consistent with this premise, Cave et al. recently assessed EPA and DHA intake in the U.S. according to ethnicity, education, and income using 2003–2014 NHANES data and found that overall, EPA+DHA intake was low, with an average daily intake of 100 mg (69). ω-3 PUFA deficiency can be corrected and DHA and EPA incorporation into tissue phospholipids increased by consuming dietary supplements made from fish or microalgal oil (70). Accordingly, to attain the tissue concentrations of DHA and EPA associated with delayed progression of autoimmunity in the present preclinical study, a patient with lupus would likely need to consume dietary supplements containing marine ω-3 PUFAs.

Strengths of this study included the use of a widely employed lupus-prone mouse model, an established human autoimmune trigger, and physiologically relevant doses of DHA. There were, however, some limitations that will require extra attention in future studies. Since it is possible that DHA supplementation affected pulmonary inflammation and AAb responses in Cohort

1 earlier than 13 week PI, the inclusion of earlier timepoints would have been useful to better understand the temporal effects of this intervention. Additionally, since DHA consumption was found to dose-dependently increase DHA, and to a lesser extent, EPA, in the plasma, lung, and kidney, it is difficult to know the extent to which this latter ω-3 PUFA contributes to amelioration of the autoimmune response. This can be addressed in the future by conducting analogous studies on the effects of EPA supplementation on cSiO2-triggered murine lupus. Also, while gene expression was assessed in the lung, measuring mRNA expression in the spleen and kidney could further expand our understanding of how DHA influenced inflammatory and autoimmune gene signatures in the systemic and renal compartments, respectively. Lastly, characterization of immune/inflammatory cell populations in the lung and kidney using additional immunohistochemical markers for T and B cell subsets, flow cytometry, and/or single cell RNA sequencing could provide further insight into how DHA intervention affected lymphoid and myeloid cells involved in inflammation and autoimmunity.

Taken together, in addition to its previously reported preventive effects of DHA supplementation against $cSiO_2$ -triggered lupus in NZBWF1, the present therapeutic dietary regimen offers promise for suppressing progression established autoimmunity and minimizing the number and severity of lupus flares following respiratory exposures to this commonly encountered occupational dust, or other inhaled environmental toxicants.

DATA AVAILABILITY STATEMENT

The raw data supporting the conclusions of this article will be made available by the authors, without undue reservation.

ETHICS STATEMENT

The animal study was reviewed and approved by the Institutional Animal Care and Use Committee at Michigan State University (AUF #01/15-021-00).

AUTHOR CONTRIBUTIONS

JP: study design, coordination, oversight, funding acquisition, manuscript preparation, and submission. PA: study design, feeding study, necropsy, immunohistochemical analyses and morphometry, and manuscript preparation. KW and LR: data curation, data analysis/interpretation, figure preparation, and manuscript writing. MB: study design, animal handling, feeding study, funding acquisition, and manuscript editing. KG: animal handling, feeding study, necropsy, lab analyses, and manuscript editing. JW: study design, necropsy, and lab analyses. RL: necropsy and lab analyses. PC: gene expression and manuscript editing. AL: fatty acid analysis and interpretation. Q-ZL: microarray, data analysis, and manuscript preparation. JH: study design, lung/kidney histopathology, morphometry, and data analyses. All authors contributed to the article and approved the submitted version.

FUNDING

This research was funded by NIH ES027353 (JP), NIH F31ES030593 (KW), NIH T32ES007255 (KW), Lupus Foundation of America (JP, KW, and MB), USDA National Institute of Food and Agriculture Hatch Project 1020129 (JP), and the Dr. Robert and Carol Deibel Family Endowment (JP).

ACKNOWLEDGMENTS

The authors thank Amy Porter, Amy Allen, and Jessie Lee Neumann of the Michigan State University Laboratory for Investigative Histopathology for their assistance with the histotechnology.

SUPPLEMENTARY MATERIAL

The Supplementary Material for this article can be found online at: https://www.frontiersin.org/articles/10.3389/fimmu.2021.653464/full#supplementary-material

REFERENCES

1. Moulton VR, Suarez-Fueyo A, Meidan E, Li H, Mizui M, Tsokos GC. Pathogenesis of human systemic lupus erythematosus: A cellular perspective. *Trends Mol Med.* (2017) 23:615–35. doi: 10.1016/j.molmed.2017.05.006
2. Parks CG, de Souza Espindola Santos A, Barbhaiya M, Costenbader KH. Understanding the role of environmental factors in the development of systemic lupus erythematosus. *Best Pract Res Clin Rheumatol.* (2017) 31:306–20. doi: 10.1016/j.berh.2017.09.005
3. Barnes H, Goh NSL, Leong TL, Hoy R. Silica-associated lung disease: An old-world exposure in modern industries. *Respirology.* (2019) 24:1165–75. doi: 10.1111/resp.13695
4. Parks CG, Cooper GS, Nylander-French LA, Sanderson WT, Dement JM, Cohen PL, et al. Occupational exposure to crystalline silica and risk of systemic lupus erythematosus: a population-based, case-control study in the southeastern United States. *Arthritis Rheum.* (2002) 46:1840–50. doi: 10.1002/art.10368
5. Pollard KM. Silica, silicosis, and autoimmunity. *Front Immunol.* (2016) 7:97. doi: 10.3389/fimmu.2016.00097
6. Morotti A, Sollaku I, Catalani S, Franceschini F, Cavazzana I, Fredi M, et al. Systematic review and meta-analysis of epidemiological studies on the association of occupational exposure to free crystalline silica and systemic lupus erythematosus. *Rheumatology.* (2020) 60:81–91. doi: 10.1093/rheumatology/keaa444
7. Brown JM, Archer AI, Pfau IC, Holian A. Silica accelerated systemic autoimmune disease in lupus-prone New Zealand mixed mice. *Clin Exp Immunol.* (2003) 131:415–21. doi: 10.1046/j.1365-2249.2003.02094.x
8. Brown JM, Pfau JC, Holian A. Immunoglobulin and lymphocyte responses following silica exposure in New Zealand mixed mice. *Inhal Toxicol.* (2004) 16:133–9. doi: 10.1080/08958370490270936
9. Brown JM, Pfau JC, Pershouse MA, Holian A. Silica, apoptosis, and autoimmunity. *J Immunotoxicol.* (2005) 1:177–87. doi: 10.1080/15476910490911922

10. Clark A, Zhao EJ, Birukova A, Buckley ES, Ord JR, Asfaw YG, et al. Inhaled silica induces autoimmunity in a strain-dependent manner. *J Immunol.* (2017) 198(1 Supplement):58.13–58.13.
11. Foster MH, Ord JR, Zhao EJ, Birukova A, Fee L, Korte FM, et al. Silica exposure differentially modulates autoimmunity in lupus strains and autoantibody transgenic mice. *Front Immunol.* (2019) 10:2336. doi: 10.3389/fimmu.2019.02336
12. Bates MA, Brandenberger C, Langohr I, Kumagai K, Harkema JR, Holian A, et al. Silica triggers inflammation and ectopic lymphoid neogenesis in the lungs in parallel with accelerated onset of systemic autoimmunity and glomerulonephritis in the lupus-prone NZBWF1 mouse. *PLoS ONE.* (2015) 10:e0125481. doi: 10.1371/journal.pone.0125481
13. Bates MA, Akbari P, Gilley KN, Wagner JG, Li N, Kopec AK, et al. Dietary docosahexaenoic acid prevents silica-induced development of pulmonary ectopic germinal centers and glomerulonephritis in the lupus-prone NZBWF1 mouse. *Front Immunol.* (2018) 9:2002. doi: 10.3389/fimmu.2018.02002
14. Borchers A, Ansari AA, Hsu T, Kono DH, Gershwin ME. The pathogenesis of autoimmunity in New Zealand mice. *Semin Arthritis Rheum.* (2000) 29:385–99. doi: 10.1053/sarh.2000.7173
15. Wierenga KA, Strakovsky RS, Benninghoff AD, Rajasinghe LD, Lock AL, Harkema JR, et al. Requisite omega-3 HUFA biomarker thresholds for preventing murine lupus flaring. *Front Immunol.* (2020) 11:1796. doi: 10.3389/fimmu.2020.01796
16. Calder PC. Omega-3 fatty acids and inflammatory processes: from molecules to man. *Biochem Soc Trans.* (2017) 45:1105–15. doi: 10.1042/bst20160474
17. Ferreira HB, Pereira AM, Melo T, Paiva A, Domingues MR. Lipidomics in autoimmune diseases with main focus on systemic lupus erythematosus. *J Pharm Biomed Anal.* (2019) 174:386–95. doi: 10.1016/j.jpba.2019.06.005
18. Akbar U, Yang M, Kurian D, Mohan C. Omega-3 fatty acids in rheumatic diseases: a critical review. *J Clin Rheum.* (2017) 23:330–9. doi: 10.1097/rhu.0000000000000563
19. Halade GV, Williams PJ, Veigas JM, Barnes JL, Fernandes G. Concentrated fish oil (Lovaza (R)) extends lifespan and attenuates kidney disease in lupus-prone short-lived (NZBxNZW)F1 mice. *Exp Bio Med.* (2013) 238:610–22. doi: 10.1177/1535370213489485
20. Halade GV, Rahman MM, Bhattacharya A, Barnes JL, Chandrasekar B, Fernandes G. Docosahexaenoic acid-enriched fish oil attenuates kidney disease and prolongs median and maximal life span of autoimmune lupus-prone mice. *J Immunol.* (2010) 184:5280–6. doi: 10.4049/jimmunol.0903282
21. Pestka JJ, Vines LL, Bates MA, He K, Langohr I. Comparative effects of n-3, n-6 and n-9 unsaturated fatty acid-rich diet consumption on lupus nephritis, autoantibody production and CD4+ T cell-related gene responses in the autoimmune NZBWF1 mouse. *PLoS ONE.* (2014) 9:e100255. doi: 10.1371/journal.pone.0100255
22. Li X, Bi X, Wang S, Zhang Z, Li F, Zhao AZ. Therapeutic potential of omega-3 polyunsaturated fatty acids in human autoimmune diseases. *Front Immunol.* (2019) 10:2241. doi: 10.3389/fimmu.2019.02241
23. Duarte-Garcia A, Myasoedova E, Karmacharya P, Hocaoglu M, Murad MH, Warrington KJ, et al. Effect of omega-3 fatty acids on systemic lupus erythematosus disease activity: A systematic review and meta-analysis. *Autoimmun Rev.* (2020) 2020:102688. doi: 10.1016/j.autrev.2020.102688
24. Charoenwoodhipong P, Harlow SD, Marder W, Hassett AL, McCune WJ, Gordon C, et al. Dietary omega polyunsaturated fatty acid intake and patient-reported outcomes in systemic lupus erythematosus: The michigan lupus epidemiology & surveillance (MILES) program. *Arthr Care Res.* (2019) 72:874–81. doi: 10.1002/acr.23925
25. Benninghoff AD, Bates MA, Chauhan PS, Wierenga KA, Gilley KN, Holian A, et al. Docosahexaenoic acid consumption impedes early interferon- and chemokine-related gene expression while suppressing silica-triggered flaring of murine lupus. *Front Immunol.* (2019) 10:2851. doi: 10.3389/fimmu.2019.02851
26. Rajasinghe LD, Li QZ, Zhu C, Yan M, Chauhan PS, Wierenga KA, et al. Omega-3 fatty acid intake suppresses induction of diverse autoantibody repertoire by crystalline silica in lupus-prone mice. *Autoimmunity.* (2020) 53:415–33. doi: 10.1080/08916934.2020.1801651
27. Reeves PG, Nielsen FH, Fahey GC, Jr. AIN-93 purified diets for laboratory rodents: final report of the American Institute of Nutrition ad hoc writing committee on the reformulation of the AIN-76A rodent diet. *J. Nutr.* (1993) 123:1939–51.
28. Biswas R, Hamilton RF, Jr., Holian A. Role of lysosomes in silica-induced inflammasome activation and inflammation in absence of MARCO. *J Immunol Res.* (2014) 2014:304180. doi: 10.1155/2014/304180
29. OSHA. *Federal Register: Occupational Exposure to Respirable Crystalline Silica*. Final Rule. (2016). Available online at: https://www.osha.gov/FedReg_osha_pdf/FED20160325B.pdf.
30. Bates MA, Brandenberger C, Langohr, II, Kumagai K, Lock AL, et al. Silica-triggered autoimmunity in lupus-prone mice blocked by docosahexaenoic acid consumption. *PLoS ONE.* (2016) 11:e0160622. doi: 10.1371/journal.pone.0160622
31. Brandenberger C, Rowley NL, Jackson-Humbles DN, Zhang Q, Bramble LA, Lewandowski RP, et al. Engineered silica nanoparticles act as adjuvants to enhance allergic airway disease in mice. *Part Fibre Toxicol.* (2013) 10:26. doi: 10.1186/1743-8977-10-26
32. Toth LA. Defining the moribund condition as an experimental endpoint for animal research. *ILAR J.* (2000) 41:72–9. doi: 10.1093/ilar.41.2.72
33. Sukhija PS, Palmquist DL. Rapid method for determination of total fatty acid content and composition of feedstuffs and feces. *J Ag Food Chem.* (1988) 36:1202–6. doi: 10.1021/jf00084a019
34. Lock AL, Preseault CL, Rico JE, DeLand KE, Allen MS. Feeding a C16:0-enriched fat supplement increased the yield of milk fat and improved conversion of feed to milk. *J Dairy Sci.* (2013) 96:6650–9. doi: 10.3168/jds.2013-6892
35. Stark KD. The percentage of n-3 highly unsaturated fatty acids in total HUFA as a biomarker for omega-3 fatty acid status in tissues. *Lipids.* (2008) 43:45–53. doi: 10.1007/s11745-007-3128-3
36. Harris WS. The omega-3 index: clinical utility for therapeutic intervention. *Curr Cardiol Rep.* (2010) 12:503–8. doi: 10.1007/s11886-010-0141-6
37. Yu F, Haas M, Glassock R, Zhao MH. Redefining lupus nephritis: clinical implications of pathophysiologic subtypes. *Nat Rev Nephrol.* (2017) 13:483–95. doi: 10.1038/nrneph.2017.85
38. Vandesompele J, De Preter K, Pattyn F, Poppe B, Van Roy N, De Paepe A, et al. Accurate normalization of real-time quantitative RT-PCR data by geometric averaging of multiple internal control genes. *Genome Biol.* (2002) 3:34. doi: 10.1186/gb-2002-3-7-research0034
39. Li QZ, Zhou J, Lian Y, Zhang B, Branch VK, Carr-Johnson F, et al. Interferon signature gene expression is correlated with autoantibody profiles in patients with incomplete lupus syndromes. *Clin Exp Immunol.* (2010) 159:281–91. doi: 10.1111/j.1365-2249.2009.04057.x
40. Metsalu T, Vilo J. ClustVis: a web tool for visualizing clustering of multivariate data using principal component analysis and heatmap. *Nucl Acids Res.* (2015) 43:W566–70. doi: 10.1093/nar/gkv468
41. Metherel AH, Chouinard-Watkins R, Trépanier MO, Lacombe RJS, Bazinet RP. Retroconversion is a minor contributor to increases in eicosapentaenoic acid following docosahexaenoic acid feeding as determined by compound specific isotope analysis in rat liver. *Nutr Metab.* (2017) 14:75. doi: 10.1186/s12986-017-0230-2
42. Bates MA, Benninghoff AD, Gilley KN, Holian A, Harkema JR, Pestka JJ. Mapping of dynamic transcriptome changes associated with silica-triggered autoimmune pathogenesis in the lupus-prone NZBWF1 mouse. *Front Immunol.* (2019) 10:632. doi: 10.3389/fimmu.2019.00632
43. Wierenga KA, Harkema JR, Pestka JJ. Lupus, silica, and dietary omega-3 fatty acid interventions. *Toxicol Pathol.* (2019) 47:1004–11. doi: 10.1177/0192623319878398
44. Kawasaki H. A mechanistic review of silica-induced inhalation toxicity. *Inhal Toxicol.* (2015) 27:363–77. doi: 10.3109/08958378.2015.1066905
45. Joshi GN, Gilberti RM, Knecht DA. Single cell snalysis of phagocytosis, phagosome maturation, phagolysosomal leakage, and cell death following exposure of macrophages to silica particles. *Meth Mol Biol.* (2017) 1519:55–77. doi: 10.1007/978-1-4939-6581-6_5
46. Desai J, Foresto-Neto O, Honarpisheh M, Steiger S, Nakazawa D, Popper B, et al. Particles of different sizes and shapes induce neutrophil necroptosis followed by the release of neutrophil extracellular trap-like chromatin. *Sci Rep.* (2017) 7:15003. doi: 10.1038/s41598-017-15106-0

47. Hamilton RF, Jr., Thakur SA, Mayfair JK, Holian A. MARCO mediates silica uptake and toxicity in alveolar macrophages from C57BL/6 mice. *J Biol Chem.* (2006) 281:34218–26. doi: 10.1074/jbc.M605229200
48. Lescoat A, Ballerie A, Lelong M, Augagneur Y, Morzadec C, Jouneau S, et al. Crystalline silica impairs efferocytosis abilities of human and mouse macrophages: implication for silica-associated systemic sclerosis. *Front Immunol.* (2020) 11:219. doi: 10.3389/fimmu.2020.00219
49. Cucchi D, Camacho-Muñoz D, Certo M, Niven J, Smith J, Nicolaou A, et al. Omega-3 polyunsaturated fatty acids impinge on CD4+ T cell motility and adipose tissue distribution via direct and lipid mediator-dependent effects. *Cardiovasc Res.* (2020) 116:1006–20. doi: 10.1093/cvr/cvz208
50. Davidson A. What is damaging the kidney in lupus nephritis? *Nature Rev Rheuma.* (2016) 12:143–53. doi: 10.1038/nrrheum.2015.159
51. Tucci M, Stucci S, Strippoli S, Silvestris F. Cytokine overproduction, T-cell activation, and defective t-regulatory functions promote nephritis in systemic lupus erythematosus. *J Biomed Biotech.* (2010) 2010:457146. doi: 10.1155/2010/457146
52. Lands B, Bibus D, Stark KD. Dynamic interactions of n-3 and n-6 fatty acid nutrients. *Prostaglandins Leukot Essent Fatty Acids.* (2018) 136:15–21. doi: 10.1016/j.plefa.2017.01.012
53. Harris WS. The Omega-6:Omega-3 ratio: A critical appraisal and possible successor. *Prostaglandins Leukot Essent Fatty Acids.* (2018) 132:24–40. doi: 10.1016/j.plefa.2018.03.003
54. Wong SW, Kwon MJ, Choi AM, Kim HP, Nakahira K, Hwang DH. Fatty acids modulate Toll-like receptor 4 activation through regulation of receptor dimerization and recruitment into lipid rafts in a reactive oxygen species-dependent manner. *J Biol Chem.* (2009) 284:27384–92. doi: 10.1074/jbc.M109.044065
55. Norris PC, Dennis EA. Omega-3 fatty acids cause dramatic changes in TLR4 and purinergic eicosanoid signaling. *Proc Natl Acad Sci USA.* (2012) 109:8517–22. doi: 10.1073/pnas.1200189109
56. Norris PC, Dennis EA. A lipidomic perspective on inflammatory macrophage eicosanoid signaling. *Adv Biol Regul.* (2014) 54:99–110. doi: 10.1016/j.jbior.2013.09.009
57. Li X, Yu Y, Funk CD. Cyclooxygenase-2 induction in macrophages is modulated by docosahexaenoic acid via interactions with free fatty acid receptor 4 (FFA4). *FASEB J.* (2013) 27:4987–97. doi: 10.1096/fj.13-235333
58. Yan Y, Jiang W, Spinetti T, Tardivel A, Castillo R, Bourquin C, et al. Omega-3 fatty acids prevent inflammation and metabolic disorder through inhibition of NLRP3 inflammasome activation. *Immunity.* (2013) 38:1154–63. doi: 10.1016/j.immuni.2013.05.015
59. Ricote M, Glass CK. PPARs and molecular mechanisms of transrepression. *Biochim Biophys Acta.* (2007) 1771:926–35. doi: 10.1016/j.bbalip.2007.02.013
60. Chang HY, Lee HN, Kim W, Surh YJ. Docosahexaenoic acid induces M2 macrophage polarization through peroxisome proliferator-activated receptor gamma activation. *Life Sci.* (2015) 120:39–47. doi: 10.1016/j.lfs.2014.10.014
61. Maderna P, Godson C. Lipoxins: resolutionary road. *Br J Pharmacol.* (2009) 158:947–59. doi: 10.1111/j.1476-5381.2009.00386.x
62. Christie WW, Harwood JL. Oxidation of polyunsaturated fatty acids to produce lipid mediators. *Essays Biochem.* (2020) 64:401–21. doi: 10.1042/ebc20190082
63. Chiang N, Fredman G, Backhed F, Oh SF, Vickery T, Schmidt BA, et al. Infection regulates pro-resolving mediators that lower antibiotic requirements. *Nature.* (2012) 484:524–8. doi: 10.1038/nature11042
64. Fredman G, Hellmann J, Proto JD, Kuriakose G, Colas RA, Dorweiler B, et al. An imbalance between specialized pro-resolving lipid mediators and pro-inflammatory leukotrienes promotes instability of atherosclerotic plaques. *Nat Commun.* (2016) 7:12859. doi: 10.1038/ncomms12859
65. Chiurchiù V, Leuti A, Dalli J, Jacobsson A, Battistini L, Maccarrone M, et al. Proresolving lipid mediators resolvin D1, resolvin D2, and maresin 1 are critical in modulating T cell responses. *Sci Transl Med.* (2016) 8:353ra111. doi: 10.1126/scitranslmed.aaf7483
66. Crouch MJ, Kosaraju R, Guesdon W, Armstrong M, Reisdorph N, Jain R, et al. Frontline science: a reduction in DHA-derived mediators in male obesity contributes toward defects in select B cell subsets and circulating antibody. *J Leukoc Biol.* (2019) 106:241–57. doi: 10.1002/jlb.3hi1017-405rr
67. EFSA Panel on Dietetic Products Allergies. Scientific Opinion on the extension of use for DHA and EPA-rich algal oil from Schizochytrium sp. as a Novel Food ingredient. *EFSA J.* (2014) 12:3843. doi: 10.2903/j.efsa.2014.3843
68. Calder PC. Omega-3 polyunsaturated fatty acids and inflammatory processes: nutrition or pharmacology? *Br J Clin Pharmacol.* (2013) 75:645–62. doi: 10.1111/j.1365-2125.2012.04374.x
69. Cave C, Hein N, Smith LM, Anderson-Berry A, Richter CK, Bisselou KS, et al. Omega-3 long-chain polyunsaturated fatty acids intake by ethnicity, income, and education level in the United States: NHANES 2003-2014. *Nutrients.* (2020) 12:7. doi: 10.3390/nu12072045
70. Walker RE, Jackson KH, Tintle NL, Shearer GC, Bernasconi A, Masson S, et al. Predicting the effects of supplemental EPA and DHA on the omega-3 index. *Am J Clin Nutr.* (2019) 110:1034–40. doi: 10.1093/ajcn/nqz161

Conflict of Interest: The authors declare that the research was conducted in the absence of any commercial or financial relationships that could be construed as a potential conflict of interest.